Ann. Rev. Astron. Astrophys. 1979. 17: 241–74

GLOBULAR CLUSTERS IN GALAXIES

William E. Harris
Department of Physics, McMaster University, Hamilton, Canada

René Racine
Département de physique, Université de Montréal, Montréal, Canada

INTRODUCTION

Globular clusters are among the most versatile of astronomical objects. Within our own Galaxy, they play central roles in galactic structure, the evolution of low-mass and metal-poor stars, the dynamics of stellar systems, the early chemical and dynamical history of the Galaxy, stellar pulsation, and most recently the nature of certain X-ray sources. But as remnants of the earliest (?) star formation epoch, they are also believed to occur almost universally in galaxies of sufficient size. The purpose of this review is to assess current knowledge about globular-cluster systems viewed as subsystems of their parent galaxies.

Modern understanding of the structure of the Galactic globular-cluster system begins with the classic studies of Shapley (1918), and knowledge of clusters in distant galaxies (M31 and beyond) dates from the equally monumental work of Hubble (1932). Despite this honorable history, detailed photometric and spectroscopic studies of clusters in any galaxies more distant than the Magellanic Clouds have taken place only in the last decade, largely because of the imposing observational problem of measuring extremely faint and small clusters superimposed on the backgrounds of large galaxies. This subject, then, is a young one and is seen here in a phase of rapid development. We shall be concerned primarily with what cluster systems have revealed about the structure, chemical composition, and extent of galaxy haloes, their intrinsic luminosity and color distribution, the kinematics of cluster systems, and the sizes of total cluster populations as functions of galaxy size and type. Inevitably, we must bypass any discussion of the wealth of data specifically on individual clusters.

0066-4146/79/0915-0241$01.00

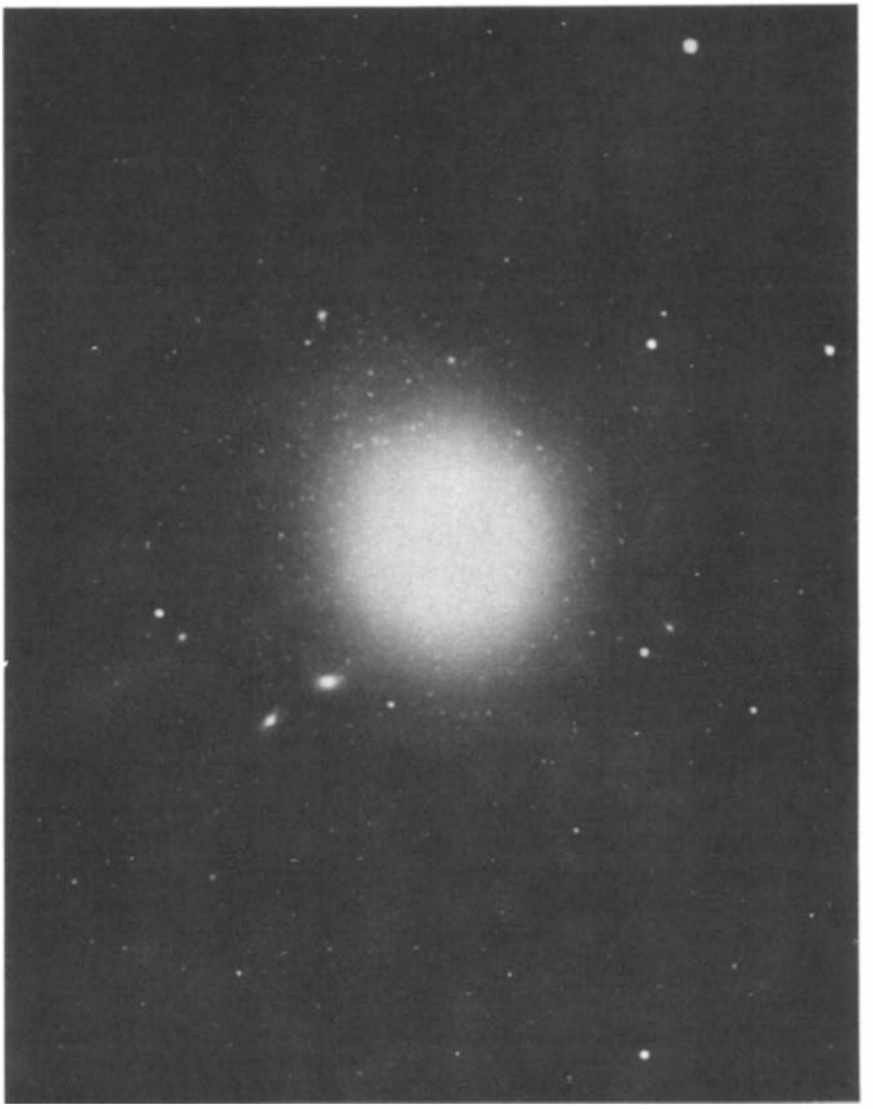

Figure 1 The largest system of globular clusters known, in the giant elliptical galaxy M87. The reproduction is from a 45-minute exposure on IIIaJ + GG385, taken by M. G. Smith with the 4-meter telescope at Cerro Tololo.

In the subsequent sections, we first discuss the compilation of data for each known globular-cluster system in turn, beginning with our own Galaxy and proceeding outward. In the final section we synthesize several integrated properties of the various known cluster systems. We shall find that, despite some significant differences, systems of globular clusters are much more similar to one another than are their parent galaxies.

1 THE GALAXY

1.1 *Fundamental Data*

The cluster system in our own Galaxy remains the one for which most complete knowledge exists, and provides the basis of comparison for all other systems. In Table 1 we summarize in catalog form the raw data relevant to this review for the 131 known Galactic globular clusters. The tabular data—which form the most important material of this section—are described below.

Columns 1–4 Cluster identification (NGC or other number, and commonly used name if any), and galactic coordinates (l,b) in degrees. The identification list follows Kukarkin (1974) with the addition of clusters 0423-21 (Schuster & West 1977) and 1730-33 (Liller 1977).

Column 5 Apparent visual distance modulus $(m–M)_V$ taken from the compilation of Harris (1976), with several significant more recent changes and additions; sources for these are given below the table. Distances for 78 clusters are now based exclusively on color-magnitude diagrams, and the others on secondary methods (Harris 1976). All are reduced to the same homogeneous system of Harris, assuming $M_V(\mathrm{HB}) = 0.6$ for the horizontal branch in all clusters.

Column 6 Integrated absolute magnitude $M_V = V_t - (m–M)_V$ where V_t is the total apparent magnitude of the cluster in the sense defined by Peterson & King (1975). Here, we collected anew all available photoelectric concentric-aperture magnitude measurements $V(r)$ for each cluster (sources given in the table), and fitted them to the King (1966a) structural curves to obtain V_t. This could be done for a total of 92 clusters. For six clusters entirely without useful photoelectric magnitudes, we adopted the photographic m_{pg} data of Christie (1940) and Sawyer & Shapley (1927) transformed into the photoelectric scale. Finally, for the sparse objects Pal 3, 4, 5, 12, and 13 the integrated magnitudes and colors were obtained by direct addition of stars from the color-magnitude diagrams.

Columns 7–8 Integrated apparent colors of the clusters in the *UBV* system. The intrinsic colors are known to be approximate indicators

Table 1 Fundamental data for Galactic globular clusters

NGC	Name	l	b	$(m-M)_V$[a]	M_V[b]	$B-V$[b]	$U-B$[b]	E_{B-V}	R	[Fe/H][c]	$\log r_t$	c	v_{LSR}[d]
104	47 Tuc	305.9	-44.9	13.46	-9.43	0.89	0.37	0.04	8.2	-0.44	1.64	2.03	-21
288		149.7	-89.4	14.70	-6.60	0.66	0.09	0.03	12.3	-1.41	1.19	0.99	-47
362		301.5	-46.3	14.90	-8.32	0.76	0.14	0.04	10.2	-1.20	1.01	1.70	218
1261		270.6	-52.1	15.70	-7.32	0.70	0.14	0.02	16.1	-1.24	0.90	1.30	41
Pal 1		130.0	19.1	18.7:				0.12	52.0:	-1.9:	0.7:	1.50	10
0423-21	Eridanus	251.1	-41.3					0.03					
Pal 2		170.5	-9.0			1.9:	1.8:	1.2:			0.67		-140
1851		244.5	-35.0	15.40	-8.10	0.78	0.22	0.07	16.4	-1.29	0.91	1.83	299
1904	M79	227.2	-29.3	15.65	-7.65	0.63	0.03	0.01	20.0	-1.58	1.03	1.60	181
2298		245.6	-16.0	15.80	-6.40	0.73	0.19	0.11	17.9	-1.41	0.86:	1.2:	48
2419		180.4	25.3	19.94	-9.57	0.66	0.07	0.03	101.3	-2.00	1.03	1.41	-23
2808		282.2	-11.3	15.52	-9.22	0.93	0.29	0.22	11.5	-1.09	1.15	1.75	89
Pal 3		240.3	41.9	20.0:	-5.3:			0.03	99.4:	-2.2:	0.63	0.97	3
3201		277.2	8.6	14.15	-7.40	0.98	0.37	0.21	9.7	-1.26	1.56	1.52	478
Pal 4		202.3	71.8	19.85	-5.65	0.80		0.00	96.3	-2.4:	0.49	0.76	157
4147		252.9	77.2	16.28	-6.02	0.60	0.07	0.02	20.2	-1.77	0.86	1.51	174
4372		301.0	-9.9	14.90	-7.10	0.97:	0.32	0.45	7.8	-1.7:	1.5:		59
4590	M68	299.6	36.0	15.01	-6.81	0.63	0.04	0.03	10.2	-2.04	1.47:	1.62:	-125
4833		303.6	-8.0	14.90	-7.55	0.96	0.28	0.38	7.6	-2.15	1.08:	0.95:	197
5024	M53	333.0	79.8	16.34	-8.62	0.64	0.10	0.05	18.1	-1.85	1.34	1.67	-88
5053		335.6	79.0	16.00	-6.20	0.64	0.06	0.03	16.2	-2.09	1.14	0.75	
5139	ω Cen	309.1	15.0	13.92	-10.27	0.79	0.19	0.11	7.1	-1.6:p	1.74	1.36	224
5272	M3	42.2	78.7	15.00	-8.65	0.69	0.10	0.01	12.4	-1.57	1.59	1.90	-143
5286		311.6	10.6	15.61	-7.99	0.87	0.29	0.27	7.5	-1.38	1.08	1.75	40
5466		42.1	73.6	15.96	-6.86	0.71	0.04	0.05	15.3	-1.91	1.32	1.15	127
5634		342.2	49.3	16.90	-7.33	0.67	0.12	0.07	17.5	-1.70	0.92:	1.6:	-58
5694		331.1	30.4	17.80	-7.60	0.69	0.07	0.08	26.1	-1.91	1.18	1.78	-179
IC 4499		307.4	-20.5	17.12	-6.52	0.88	0.36:	0.24	15.4	-1.0:	1.20	1.10	
5824		332.6	22.1	17.32	-8.32	0.75	0.15	0.14	17.1	-1.67	1.30	2.51	-56
Pal 5		0.9	45.9	16.75	-5.00	0.70		0.03	16.5	-1.24	1.26:		
5897		342.9	30.3	15.60	-7.05	0.75	0.08:	0.06	6.9	-1.45	1.06	0.82	
5904	M5	3.9	46.8	14.51	-8.76	0.71	0.12	0.03	6.7	-1.25	1.46	1.78	59
5927		326.6	4.9	16.10	-7.77	1.31	0.84	0.55	5.0	-0.67	1.06:	1.45:	-85
5946		327.3	4.2	16.7:	-7.05:	1.24	0.54	0.56	5.3:	-1.5:	0.8:	1.6:	
5986		337.0	13.3	15.90	-8.78	0.90	0.30	0.27	4.5	-1.26	1.10	1.42	5
1608+15	Pal 14	28.8	42.2	19.2:				0.03	60:	-1.6:			98
6093	M80	352.7	19.5	15.28	-8.08	0.85	0.24:	0.21	3.2	-1.54	0.97	1.88	28
6101		317.7	-15.8	15.70	-6.40	0.68:	0.10	0.08	8.6	-1.8:			
6121	M4	351.0	16.0	12.73	-6.80	1.03	0.44	0.35	7.0	-1.30	1.64	1.45	73
6139		342.4	6.9	16.93:	-7.75:	1.39	0.73	0.68	3.0:	-1.27:	1.10	1.75	25
6144		351.9	15.7	15.69	-6.57	1.01	0.45	0.36	2.8	-0.9:	0.8:	0.97:	
6171	M107	3.4	23.0	15.03	-6.90	1.14	0.55	0.37	4.3	-0.79	1.36	1.50	-135
6205	M13	59.0	40.9	14.35	-8.49	0.69	0.03	0.02	9.1	-1.42	1.43	1.55	-225
6218	M12	15.7	26.3	14.30	-7.70	0.82	0.21	0.19	5.1	-1.64	1.26	1.31	21
6229		73.6	40.3	17.50	-8.07	0.71	0.05:	0.01	30.6	-1.44	0.75	1.41	-137
6235		358.9	13.5	16.31:	-6.16:	1.04	0.40	0.38	2.8:	-1.2:			
6254	M10	15.1	23.1	14.05	-7.48	0.92	0.23	0.26	5.5	-1.43	1.38	1.49	82
6256	Trz 12	347.8	3.4	16.6:		1.68	1.04						
Pal 15		18.9	24.3					0.09:					
6266	M62	353.6	7.3	15.38	-8.78	1.17	0.52	0.46	3.2	-1.14	1.03	1.63	-66
6273	M19	356.9	9.4	16.35	-9.20	1.00	0.37	0.38	2.4	-1.61	1.24	1.50	135
6284		358.4	9.9	15.89:	-6.94:	0.95	0.37	0.27	2.0:	-1.01:	1.0:	1.9:	32
6287		0.1	11.0	15.92:	-6.67:	1.20:	0.65	0.36	1.7:	-0.39:	1.15:	1.65:	
6293		357.6	7.8	15.41:	-7.21:	0.98	0.29	0.34	2.0:	-1.86:	1.2:	1.8:	-63
6304		355.8	5.4	15.50	-7.08	1.33	0.85	0.58	3.7	-0.37	1.2:	1.6:	-89
6316		357.2	5.8	16.99:	-7.99:	1.27	0.66	0.48	3.5:	-0.44:	1.25:	1.6:	
6325		1.0	8.0	16.70	-6.00	1.54:	0.88:	0.80	2.5	-0.7:	1.1:	1.6:	
6333	M9	5.5	10.7	15.34:	-7.41:	0.94	0.30	0.36	2.7:	-1.81:	1.19	1.60	236
6341	M92	68.4	34.9	14.50	-7.98	0.62	0.00	0.01	10.0	-2.12	1.22	1.78	-98
6342		4.9	9.7	17.5:	-7.60:	1.29	0.73	0.49	6.7:	-0.41	1.05:	1.6:	
6352		341.4	-7.2	14.47	-6.32	1.06	0.63	0.25	4.3	-0.06	1.05:	1.1:	
6355		359.6	5.4	16.6:	-7.00:	1.46	0.76	0.76	2.3:	-1.05:	1.15:	1.6:	
6356		6.7	10.2	17.07	-8.67	1.11	0.60	0.28	8.6	-0.37	0.92:	1.3:	45
Trz 2		356.3	2.3								0.4:		
6362		325.5	-17.6	14.65	-6.35	0.85	0.28	0.12	5.6	-0.9:	1.22	1.02	-18
6366		18.4	16.0	15.1:	-5.10:	1.47	0.98	0.65	5.6:	-0.1:	1.35:	1.45:	
Trz 4		356.0	1.3										
HP 1		357.4	2.1								0.7:		
1730-33	Liller 1	354.8	-0.2										
6380		350.3	-3.6								0.8:		
6388		345.5	-6.7	16.83	-9.98	1.17	0.66	0.32	6.3	-0.48	0.92	1.75	86
Trz 1		357.6	1.0								0.7:		
Ton 2		350.8	-3.4								0.8:		
6397		338.2	-12.0	12.30	-6.65	0.75	0.15	0.18	7.1	-1.83	1.64	1.86	20
6401		3.5	4.0	16.7:	-7.20:	1.58	0.89	0.79	2.3:	-0.7:	0.95:	1.45:	
6402	M14	21.3	14.8	16.90	-9.34	1.28	0.64	0.58	4.4	-1.28	1.00	1.10	-88
Pal 6		2.1	1.8	18.1:				1.8:	6.1:		1.1:		
6426		28.1	16.2	17.30	-6.10	1.03	0.34	0.40	9.6	-1.35:	1.0:	1.45:	
Trz 5		3.8	1.7			2.77	2.1:	1.8:			0.6:		
6440		7.7	3.8	16.40	-6.75	1.98	1.51	1.11	4.8	-0.28	0.9:	1.6:	-84

Table 1 (*continued*)

NGC	Name	l	b	$(m-M)_V$[a]	M_V[b]	$B-V$[b]	$U-B$[b]	E_{B-V}	R	[Fe/H][c]	$\log r_t$	c	v_{LSR}[d]
6441		353.5	-5.0	16.50	-9.08	1.28	0.83	0.45	1.9	-0.24	0.88	1.70	20
Trz 6		358.6	-2.2								0.4:		
6453		355.7	-4.0	16.4:	-6.50:	1.28:	0.65:	0.67:	2.1:	-1.1:	0.8:		
6496		348.1	-10.0	15.0:	-5.80:	0.93	0.42:	0.07	2.4:	-0.1:	1.1:		
Trz 9		3.6	-2.0										
6517		19.2	6.8	18.10:	-7.80:	1.79	0.94	1.14	3.2:	-1.33	1.2:	2.0:	
6522		1.0	-3.9	15.64	-7.04	1.22	0.67	0.50	2.6	-1.04	0.85:	1.45:	-17
6528		1.1	-4.2	16.40	-6.90	1.45	1.10	0.65	1.8	-0.43	0.75:	1.45:	133
6535		27.2	10.4	16.35:	-5.75:	0.97	0.31	0.36	5.3:	-1.9:	0.75:	0.7:	
6539		20.8	6.8	15.7:	-6.10:	1.89	1.10:	1.22	6.9:	-1.2:	1.35:	1.6:	
6541		349.3	-11.2	14.60	-7.96	0.77	0.14	0.13	3.0	-1.59	1.50	2.00	-142
6544		5.8	-2.2	15.35	-7.10	1.36	0.67:	0.63	4.4	-1.02	1.1:	1.45:	-1
6553		5.3	-3.1	16.40	-8.15	1.62	1.24	0.79	3.3	-0.4:	1.0:	1.2:	-18
6558		0.2	-6.0	16.1:		1.09	0.48:	0.40	1.0:	-0.9:	0.8:		
IC 1276	Pal 7	21.8	5.7	18.50		1.74	1.0:	0.92	5.8	-0.8:	1.1:		
Trz 11		8.4	-2.2										
6569		0.5	-6.7	16.47:	-7.77:	1.34	0.63	0.63	1.6:	-0.54:	1.0:	1.45:	
6584		342.1	-16.4	16.17:	-6.99:	0.79	0.17	0.11	7.3:	-1.40	0.75:	1.2:	164
6624		2.8	-7.9	15.45	-7.13	1.10	0.57	0.25	1.4	-0.34	0.8:	1.2:	79
6626	M26	7.8	-5.6	14.99:	-8.06:	1.10	0.45	0.33	3.1:	-1.08	1.2:	1.6:	12
6637	M69	1.7	-10.3	15.60	-7.90	0.99	0.50	0.17	2.2	-0.47	1.0:	1.45:	68
6638		7.9	-7.2	15.66:	-6.51:	1.16	0.58	0.36	1.9:	-0.6:	0.77	1.30	-3
6642		9.8	-6.4	15.11		1.08	0.50:	0.36	3.2	-0.88:	0.9:		-75
6652		1.5	-11.4	16.23:	-7.32:	0.92	0.39	0.11	6.4:	-0.5:	0.8:	1.45:	-115
6656	M22	9.9	-7.6	13.55	-8.45	0.99	0.30	0.35	6.1	-1.69	1.52	1.24	-132
Pal 8		14.1	-6.8	18.4:		1.19	0.69:	0.30	22:		0.9:		
6681	M70	2.9	-12.5	15.40	-7.32	0.71	0.14	0.07	2.9	-1.17	1.05:	1.1:	208
6712		25.3	-4.3	15.51	-7.30	1.16	0.56	0.35	4.0	-0.43	1.1:	1.2:	-111
6715	M54	5.6	-14.1	17.11	-9.41	0.85	0.24	0.14	13.0	-1.55	0.87	1.85	132
6717	Pal 9	12.9	-10.9	16.55:		0.93	0.37	0.18	7.5:		0.8:		
6723		0.1	-17.3	14.80	-7.48	0.75	0.24	0.03	2.7	-0.85	1.10	1.20	5
6749		36.1	-2.2			1.76:	0.74:	0.96:			0.7:	1.2:	
6752		336.5	-25.6	13.20	-7.80	0.65	0.07	0.03	6.0	-1.62	1.54	1.84	-37
6760		36.1	-3.9	15.90	-6.80	1.66	1.00:	0.91	6.3	-1.06	1.03:	1.45:	
Trz 7		3.4	-20.0					0.12:					
6779	M56	62.7	8.3	15.60	-7.35	0.86	0.18	0.22	9.7	-1.79	1.0:	1.4:	-126
Pal 10		52.4	2.7	18.6:				1.2:	7.9:		0.8:		
1925-30		8.6	-20.8					0.11:			0.8:		
6809	M55	8.8	-23.3	13.80	-6.85	0.69	0.10	0.07	4.8	-1.78	1.27	1.03	178
Pal 11		31.8	-15.6	16.40				0.35:	6.7	-0.63	0.87	0.75	-54
6838	M71	56.7	-4.5	13.90	-5.60	1.13	0.54	0.28	7.6	-0.28	1.1:	1.2:	-1
6864	M75	20.3	-25.8	16.85	-8.30	0.87	0.28	0.17	11.7	-1.30	0.82	1.78	-187
6934		52.1	-18.9	16.22	-7.34	0.74	0.19	0.12	12.0	-1.38	0.95	1.35	-345
6981	M72	35.2	-32.7	16.29	-6.94	0.72	0.13	0.03	12.9	-1.27	0.94	1.19	-244
7006		63.8	-19.4	18.12	-7.52	0.74	0.17	0.13	32.1	-1.66	0.80	1.38	-371
7078	M15	65.0	-27.3	15.26	-8.91	0.68	0.06	0.12	10.3	-2.01	1.32	1.96	-97
7089	M2	53.4	-35.8	15.45	-8.95	0.67	0.08	0.06	10.5	-1.53	1.21	1.61	0
7099	M30	27.2	-46.8	14.60	-7.10	0.58	0.03	0.01	7.6	-2.03	1.20	2.11	-172
Pal 12		30.5	-47.6	16.46	-4.30	0.90	0.29:	0.02	15.6	-1.55	0.90	0.75	15
Pal 13		87.1	-42.7	17.10	-2.60	0.69:	-0.14:	0.05	25.7	-2.03	0.5:		-22
7492		53.3	-63.5	16.70	-5.20	0.48	0.17:	0.00	21.3	-2.0:	0.88	0.98	
Error				0.3	0.1	0.02	0.03	0.04	15%	0.2	0.1	0.2	20

Additional sources of compiled data:

[a] Distance moduli: Alcaino 1977a, 1978a; Canterna & Schommer 1978; Diamond 1976; Harris 1977, 1978; Harris & Canterna 1979a; Harris & Hesser 1976; Hartwick & Sargent 1978; Hesser et al. 1977; Lee 1977a,b,c; Liller & Carney 1978; Rutily & Terzan 1977; Sandage & Hartwick 1977; Sandage et al. 1977; Searle & Zinn 1978.

[b] Aperture photometry: Bernard 1976; Corwin 1977; Gascoigne & Burr 1956; Harris & van den Bergh 1974; Illingworth 1976; Johnson 1959; King 1966b; Kron 1966, 1975; Kron & Mayall 1960; Racine 1975; Rousseau 1964; van den Bergh 1967, 1971, 1977a; van den Bergh & Hagen 1968; Zaitseva et al. 1974.

[c] Heavy-element abundances: Bell & Gustafsson 1976; Butler 1975; Canterna & Schommer 1978; Cohen 1978; Cowley et al. 1978; Harris 1978; Harris & Canterna 1979b; Helfer et al. 1959; Hesser et al. 1977 and references cited; Mallia 1977; Searle & Zinn 1978.

[d] Radial velocities: Da Costa et al. 1977; Gratton & Nesci 1978; Hartwick & Sargent 1978; Jenner & Kwitter 1977; Kinman 1959a; Mayall 1946; Smith et al. 1976; van den Bergh 1969; Zinn 1974.

of cluster metallicity, and for most of the extragalactic cluster systems, only the broadband colors are available to provide heavy-element abundance estimates. Here, all available photoelectric *UBV* measurements have again been correlated and averaged into a completely new list (sources as in Column 6 above).

Column 9 Foreground reddening $E(B-V)$, from Harris (1976) or the individual color-magnitude studies. For several remaining clusters a cosecant-law estimate $E(B-V) = 0.06\ (\csc |b| - 1)$ was used.

Column 10 Galactocentric distance R, in kpc. We assume the Sun to be 9.0 kpc from the Galactic center (Harris 1976), and the ratio $A_V/E(B-V) = 3.2$.

Column 11 Estimate of the heavy-element abundance of each cluster, $[\mathrm{Fe/H}] \equiv \log (\mathrm{Fe/H})_{\mathrm{cl}} - \log (\mathrm{Fe/H})_{\odot}$. Where possible, these are based on averages of abundance determinations from individual cluster giants; primary references are given in the table. The relations between [Fe/H], integrated spectral type, and integrated broadband colors (Harris & Canterna 1977, 1979b, Kron & Guetter 1976) were used to derive less precise [Fe/H] estimates on the same scale for the other clusters.

Columns 12–13 The King (1966a) structural parameters: tidal radius r_t in arc min and central concentration $c = \log (r_t/r_c)$. These are taken for 105 clusters either from the extensive star-count data of Peterson & King (1975) and Peterson (1976), or from our own application of the King (1966a) curves to the concentric-aperture photometry (Column 6 above) to derive r_t and r_c. For 18 remaining objects we have taken r_t as transformed from Kukarkin (1974), although these are not used in subsequent calculations as they were obtained originally on different scales.

Column 14 The radial velocity v_{LSR}, reduced to the Local Standard of Rest (peculiar solar motion adopted as 20 km s^{-1} toward $l = 57°$, $b = 22°$; cf Delhaye 1965). Sources are as given in Table 1; we have not included the important but as yet incomplete new southern survey of J. E. Hesser & S. J. Shawl, which should yield major improvements in the velocity data for many clusters.

Because of the wealth of new data in almost every category, Table 1 is intended, where applicable, to replace earlier catalogues (e.g. Sawyer Hogg 1959, Arp 1965, Kukarkin 1974, Peterson & King 1975, Woltjer 1975, Harris 1976, Alcaino 1977b). But despite the dramatic current observational gains, the many blank or uncertain entries in Table 1 testify to the amount of fundamental work still needed. At the end of Table 1 we have listed internal errors for each column. These are not meant to

apply rigorously to each cluster, but are simply our estimates of the typical reliability of each quantity. Values marked with colons are regarded as more uncertain than the quoted error by a factor of two or more.

1.2 *Population and Space Distribution*

The 131 objects in Table 1 can hardly make up all globular clusters now present in the Galaxy, both because many objects in the Galactic center region must be obscured from (optical) view and because the sky has not yet been completely searched for distant Palomar-type clusters. Recent discussions (Harris 1976, Oort 1977) conclude that the central regions especially may be hiding $\sim$30–70 more clusters, mostly on the far side of the center, making the total population N_t (Galaxy) $\simeq$ 160–200. These estimates will remain uncertain until appropriate infrared searches in the Galactic center are completed.

The distribution of clusters through the halo, i.e. the number of clusters per unit volume, $\rho(R)$, has been extensively reviewed by Harris (1976) (see also Woltjer 1975, Sharov 1976, Oort 1977, de Vaucouleurs 1977a). Clusters of all metallicity types are strongly concentrated to the Galactic center, in roughly spherical symmetry. Harris (1976) shows that $\rho(R)$ can be described by a simple power law $\rho \sim R^{-n}$, where n gradually increases with R, from $n \simeq 3$ at $R \lesssim 10$ kpc up to $n \simeq 4$ for $R \gtrsim 40$ kpc. De Vaucouleurs (1977a) demonstrates in addition that $\rho(R)$ can also be reproduced accurately with the same type of $R^{1/4}$ law that applies to the haloes of many elliptical galaxies.

1.3 *Distribution of Physical Properties with Distance*

Early indications that certain intrinsic properties of the globular clusters (most noticeably, their integrated spectral types) changed with location in the Galaxy (Mayall 1946, Morgan 1956, Kinman 1959b) have grown into a more fully developed picture of cluster heavy-element abundance as a function of distance R. Recent discussions of this topic, with conflicting conclusions, are found in Harris (1976), Canterna & Schommer (1978), Cowley et al. (1978), Searle & Zinn (1978), Searle (1978), and Harris & Canterna (1979b). Although it is clear that the most metal-rich clusters ([Fe/H] > -1) can be found only in the inner halo ($R < 8$ kpc), a point of current dispute is whether the average cluster metallicity or range in [Fe/H] at a given R continues to decrease outward to the limits of the system. The abundance structure of the halo provides a basic test of protogalactic enrichment models (Larson 1976, Hartwick 1976, Searle & Zinn 1978).

The relevant data ([Fe/H] vs R from Table 1) are displayed in Figure 2. Though better observations for more outlying clusters are urgently needed to fill in the region $R > 20$ kpc, it is plain that the maximum [Fe/H] decreases roughly linearly with log R, even out to ~ 100 kpc. But even at the largest distances, a noticeable range of abundances and line strengths still appears to be present (Cowley et al. 1978, Canterna & Schommer 1978). Little can be said of the true minimum [Fe/H] vs R, since few abundance indicators used to date are sensitive to variations in [Fe/H] at such low metallicity; thus previous suggestions that $[Fe/H]_{min}$ remains roughly constant with R (Harris 1976) may prove invalid. Nevertheless, the lack of any known super-metal-poor objects with $[Fe/H] \lesssim -3$, —the fabled "Population III"—remains an intriguing problem.

The fairest summary of the current abundance-gradient situation may be that (*a*) both the total range in cluster abundances and the maximum abundance found at any R decrease steadily outward to at least 20 kpc, and likely further, and (*b*) measurable abundance differences between clusters persist at all distances, with $[Fe/H]_{min}$ not being well defined. Table 2 summarizes these points numerically.

The internal structural properties of the clusters—their luminosities M_V (or masses), radii r_t, and central concentrations c—are tied both to the cluster formation process and to subsequent dynamical evolution.

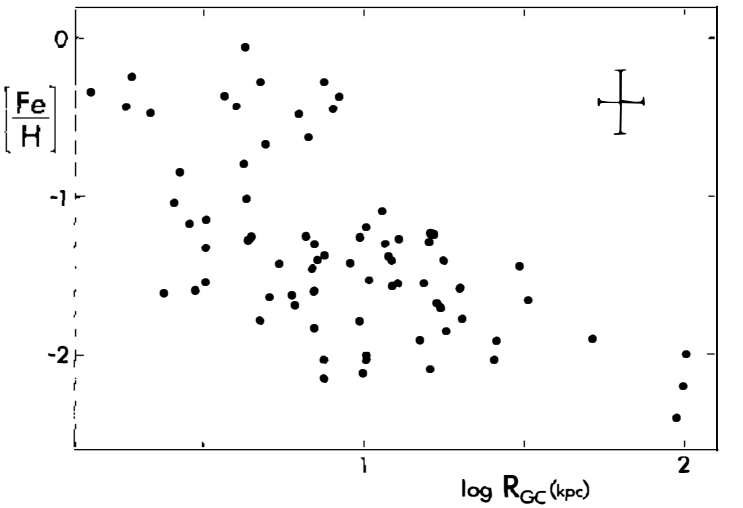

Figure 2 The relation between metallicity index [Fe/H] and galactocentric distance R_{GC} for globular clusters in the Galaxy. The typical internal errors for each point (± 0.2 in [Fe/H], $\pm 0^m.3$ in distance modulus) are indicated at upper right.

Table 2 Mean physical properties of Galactic globular clusters[a]

R (kpc)	$\overline{[Fe/H]}$	$\overline{M_V}$	$\bar{c}$	$\bar{r}_t$ (pc)	$\bar{e}$
0–3	-0.91 ± 0.10 (24)	-7.20 ± 0.18 (23)	1.51 ± 0.06 (20)	29 ± 3 (20)	0.32 ± 0.07 (9)
3–6	-0.99 ± 0.11 (25)	-7.43 ± 0.20 (23)	1.42 ± 0.06 (23)	27 ± 2 (23)	0.58 ± 0.04 (16)
6–10	-1.27 ± 0.11 (26)	-7.60 ± 0.24 (25)	1.47 ± 0.07 (24)	37 ± 3 (24)	0.65 ± 0.03 (18)
10–20	-1.52 ± 0.06 (23)	-7.48 ± 0.28 (23)	1.51 ± 0.09 (22)	61 ± 7 (23)	0.58 ± 0.06 (20)
>20	-1.90 ± 0.08 (11)	-6.39 ± 0.68 (9)	1.30 ± 0.11 (9)	100 ± 26 (9)	0.55 ± 0.09 (7)
All	-1.24 ± 0.05 (109)	-7.34 ± 0.12 (103)	1.46 ± 0.03 (98)	44 ± 4 (99)	0.57 ± 0.03 (70)

[a] Quoted errors represent the formal internal standard error of the *mean*. Numbers in parentheses are the total number of clusters in the bin.

Thus one might expect *a priori* that even if clusters were formed similarly at all distances, some trend of $M_V(R)$, $r_t(R)$, etc. might develop with time as a result of tidal shocks, dynamical friction, or various other processes (Spitzer 1958, King 1962, Ostriker et al. 1972, Tremaine et al. 1975, Tremaine 1976, Oort 1977, Surdin & Charikov 1977, Keenan 1978), though the actual efficacy of dynamical friction has been questioned (van den Bergh 1978). All clusters are driven by internal dynamical relaxation toward stellar evaporation, higher central concentration, and internal stratification of stars by mass (for comprehensive reviews with references, see Lightman & Shapiro 1978 and Saslaw 1973).

Clusters now near the Galactic center also have shorter core-relaxation times (van den Bergh 1978, King 1978b). The overall result of all these effects, over sufficient time, would be to flatten out the central $\rho(R)$ distribution as well as to change the mean cluster luminosity at different distances.

Interestingly, in reality few trends with R are evident within our own Galaxy aside from the obvious ones that the inner clusters tend to have systematically smaller core and tidal radii, and that the extremely sparse Palomar-type objects are presently found only at large distances. No strong trends with R are found in the central concentration c, or in the mean cluster luminosity $\bar{M}_V$ or detailed luminosity function $\phi(M_V)$. This latter point bears on the practical question of the universality of the globular-cluster luminosity distribution depending on what region of the halo or what type of galaxy is studied (Section 6.2 below).

1.4 *Kinematics and Orbital Characteristics*

A long-standing problem has been to estimate the true sizes and eccentricities of globular-cluster *orbits* (Kurth 1960, Schmidt 1956, von Hoerner 1955, Kinman 1959c, Matsunami 1963, Innanen 1967, Peterson 1974, Racine & Harris 1975, House & Wiegandt 1977). Since cluster-cluster encounters are too rare to produce any internal relaxation of the

system over 10^{10} yr (Woolley 1961), the present distribution of cluster orbits should be close to that prevailing at their formation, except possibly in the very central regions and the disk, where dynamical friction may regularize the orbits (Tremaine et al. 1975, Keenan 1978). In addition, close orbital encounters with the Magellanic Clouds may be frequent enough to have altered the orbits of one or two outer clusters drastically (Innanen & Valtonen 1977).

In general, no complete solution for the orbit of a given cluster is possible since the tangential velocity is usually unknown. A statistical approach (Peterson 1974) can be used to calculate the most probable orbital eccentricity e_p for a given cluster, knowing its present distance R, radial velocity V_r, and tidal radius r_t (and hence perigalacticon distance R_p). Peterson (cf his Figure 4), using the Schmidt (1965) mass model and data for 30 clusters, found an average $\bar{e}_p = 0.64$ with dispersion $\sigma_e \simeq 0.2$. Thus, few clusters have extremely large or small eccentricities, with 2/3 in the middle range $0.4 < e_p < 0.8$. Matsunami (1963) and House & Wiegandt (1977) reached similar conclusions from somewhat different approaches. For the 49 clusters in Table 1 with accurate (R, r_t) we find results for $\bar{e}_p$ and σ_e virtually identical to Peterson's, by using a simple point-mass model for the Galaxy following Hartwick & Sargent (1978).

Although the foregoing method is preferred for estimating the orbit of an individual object, the mean results can be checked by a second, velocity-independent approach. For any elliptical orbit of semimajor axis a and eccentricity e, the time-averaged mean distance $\bar{R}$ from the galactic center is $\bar{R} = R_p(1 + \frac{1}{2}e^2)/(1 - e)$ (van de Kamp 1964). We may then blindly assume for every cluster that $\bar{R} \simeq R$ (now) and solve for e, knowing R_p. Over a sufficient sample of clusters the average $\bar{e}$ thus obtained will be a valid estimate for the group (after adding a second-order correction to account for the nonuniform spread of time intervals spent on each part of an elliptical orbit). We can apply this method to seventy clusters. Our results for $\bar{e}$, broken into distance groups, are summarized in Table 2. No significant trends with metallicity are found ($\bar{e} = 0.52 \pm 0.06$ for 17 clusters with $[\text{Fe/H}] > -1$, and 0.57 ± 0.03 for 53 more metal-poor clusters). We further find that $\bar{e}$ does not vary with distance R except for the (uncertain) innermost group where it is about half as large. If real, this latter difference may indicate the stronger "smoothing" effect of dynamical friction on orbits near the center, or a slightly later dynamical epoch of formation where the collapsing gas had settled into less eccentric orbits.

Both approaches suggest that a typical globular-cluster orbit has $\bar{e} \sim 0.6$ almost independent of distance. Although this eccentricity is appreciable, it should not be thought of as representing a "nearly rectilinear," plunging

orbit as in the viewpoint of Eggen et al. (1962): with $e = 0.6$, the major/minor axial ratio is still only $a/b \simeq 4/3$. The statement $\bar{e}(R) \sim$ constant also has the interesting consequence that the angular momentum per unit mass h carried by individual clusters increases outward, since $h^2 = G\mathcal{M}_{gal}R_p(1+e)$. If $\mathcal{M}_{gal}$ increases roughly as $R^{0.5-1.0}$ (see below), then $h \propto R^{1/2}$. This qualitative effect is predicted in the protogalaxy models of Larson (1975, 1976), in which gas cloud collisions within the collapsing galaxy create a net outward transport of angular momentum until star formation is largely complete.

The *kinematics* of the cluster systems have also been frequently discussed (Schmidt 1956, Arp 1965, Woltjer 1975, and especially Kinman 1959c), the most complete up-to-date treatment being by Hartwick & Sargent (1978). Their results confirm earlier conclusions that the system possesses differential rotation: the inner, more metal-rich subsystem has a significantly higher overall rotation speed. But virtually all parts of the system appear to have at least some rotation relative to an external rest frame, if the orbital speed of the Sun in the Galaxy is 200–250 km s^{-1}. A possible reason for why we do not see any obvious rotational flattening of the inner subsystem (Harris 1976) has been discussed by Woolley (1961).

Hartwick & Sargent (1978) have also used their new radial-velocity measures for the outer Palomar and dwarf spheroidal systems to investigate the velocity dispersion of the cluster system and hence the mass of the Galaxy at different R. Depending on assumptions about the velocity ellipsoid (orbit eccentricity distribution), they find $\mathcal{M}_{gal}$ increases roughly as $R^{0.5}$ or $R^{1.0}$, up to $\sim(3\text{–}10) \times 10^{11}\ \mathcal{M}_\odot$ outside 60 kpc. More simply, if $\mathcal{M}_{gal}$ within $R \simeq 30$ kpc is any less than about $4 \times 10^{11}\ \mathcal{M}_\odot$ we would face the improbable situation that at least four clusters (Pal 3, 4, NGC 1851, 5694) would have unbound orbits from their radial velocities alone. The cluster velocity data therefore provide one of the most important direct indications that the outer halo contains substantial mass. The result (several $10^{11}\ \mathcal{M}_\odot$) is an order of magnitude higher than that obtained by simply scaling up the total mass in the cluster system by the solar-neighborhood ratio of Population II field-star mass density to cluster density (Harris 1976). In turn, it casts some doubts on the frequent assumption that the density distribution of halo mass mimics the cluster distribution $\rho(R)$.

2 THE MAGELLANIC CLOUDS

The cluster populations in the Large and Small Magellanic Clouds (LMC, SMC) present unique challenges: here, we must face squarely the problem of defining a globular cluster. The rather clear population separation

between open and globular clusters within the Galaxy fails completely for the Clouds, which contain many young and intermediate-age clusters structurally similar to conventional globular clusters (Bok 1966, Freeman 1974, Gascoigne 1971, Gascoigne & Kron 1952). In general, cluster

Table 3 Globular clusters in the Magellanic Clouds

Name	V_t[a]	$(B-V)$	$(U-B)$	CMD[b]	Remarks
Large Magellanic Cloud					
NGC 1466	11.4	0.61:	0.13	√	RRLyr.; bright star superimposed
NGC 1751	11.4	0.83	0.38		
NGC 1754	11.0	0.72	0.17	–	
NGC 1786	10.1	0.76	0.14	–	
NGC 1835	9.8	0.72	0.12	–	
NGC 1841	12.6	0.72	0.04	√	
NGC 1916	9.4:	0.78	0.19	-	
NGC 1978	9.9	0.79	0.24	?	RRLyr.; carbon stars
NGC 2019	10.6	0.75	0.18	-	
NGC 2121	11.2	0.86	0.25	?	
NGC 2155	11.9	0.80	0.23	?	
NGC 2173	11.6	0.83	0.28	?	
NGC 2210	10.2	0.71	0.11	√	
NGC 2257	13.5	0.68	-	√	RRLyr.
SL-868	11.2	0.60	0.00		
Anon 14	12.7	0.72	0.20	?	
Hodge 11	12.1	0.61	−0.06	√	
Small Magellanic Cloud					
NGC 121	10.6	0.78	0.14	√	RRLyr.; carbon stars
NGC 152	12.3	0.70	0.20	–	
NGC 339	11.9	0.69	0.09	√	
NGC 361	11.8	0.76	0.14	√	
NGC 416	11.0	0.77	0.19	-	
L 1	12.0	0.72	0.21	√	
L8/K3	11.4	0.67	0.12	√	
L58/K37	14.2	0.63	-	√	
L 68	12.9	0.80	0.17	-	
L113	12.9	0.73	0.09	–	
Possible Small Magellanic Cloud candidates					
NGC 419	10.0	0.67	0.25	?	carbon stars
HC 276#81	11.2	0.77			Kron & Mayall 1960
Anon	11.5	0.69	-	-	Gascoigne & Lynga 1963

[a] Obtained by extrapolating concentric-aperture $V(r)$ photometry via the King (1966a) curves where possible, otherwise, by subtracting the mean difference $\langle V(r) - V_t \rangle$ for the given aperture sizes. The most frequently used aperture is 60″ diameter, for which $\langle V(r) - V_t \rangle = 0.7 \pm 0.1$.

[b] Color-magnitude diagram characteristics. (√): globular-cluster-like; (?): available CMD inconclusive; (–) no data available.

formation appears to have proceeded more steadily in the Clouds (particularly the LMC), and no large age gap separates the "true" globulars from the oldest open clusters, as it does in the Galaxy (Demarque & McClure 1977, van den Bergh 1975). Color-magnitude diagrams (CMD) might eventually provide definitive classification criteria but are extremely difficult to carry out in the crowded star fields of the Clouds. To date, calibrated CMDs are available for only a few LMC and SMC clusters clearly showing characteristic sequences of globular clusters (Arp 1958, Freeman & Gascoigne 1977, Gascoigne 1966, Hodge 1960b, 1971a, Tifft 1962, Walker 1970, 1972). Hesser et al. (1976) have also obtained uncalibrated but useful diagrams for numerous LMC clusters.

We have adopted integrated UBV colors as our primary classification criterion here, partly because we prefer, conservatively, to define globular clusters as restricted to the oldest group of clusters formed in any galaxy, and partly because integrated broad-band photometry is the only available criterion in still more distant galaxies (see Hartwick & Cowley 1978 for similar views). Photoelectric UBV magnitudes and colors are available for 141 LMC and 52 SMC clusters (Kron & Mayall 1960, Gascoigne 1966, van den Bergh & Hagen 1968, Bigay & Bernard 1974, Bernard 1975, 1976, Alcaino 1978b). Of these, we retained as globular-cluster candidates those with $(B-V)_0 > 0.5$ (38 in LMC, 13 in SMC). We next eliminated those whose $(U-B)$ index is >0.10 mag redder than normal for a Galactic globular of the same $(B-V)$. This leaves a final adopted list of 17 LMC and 10 SMC clusters (Table 3) which we define as most likely to be "globular" in the Galactic sense. Three additional SMC objects with insufficient or conflicting data are also listed. In Table 3, non-NGC clusters are from the lists of Lindsay (1956, 1958), Kron (1956), or Hodge (1960a). Additional references or classification criteria are listed in the last column.

All the red clusters are plotted in the two-color plane of Figure 3. Our rejected candidates (crosses in Figure 3*c*) are seen to occupy a region below the intrinsic globular line which is normally populated by old open clusters such as M67 or NGC 188 (Gray 1965, Goodenough & Hartwick 1970), so we identify them as mostly somewhat younger objects than the "true" globular clusters. Virtually all of these intermediate-age clusters are in the LMC sample; the SMC appears to contain relatively fewer of them. Despite the crudeness of our color criterion, additional tests [CMD morphology, occurrence of RR Lyrae variables, spectrophotometric indices (Danziger 1973)] yield no conflicting classifications except for NGC 1852 (colors like those of an old globular, but CMD unlike one). As yet, virtually no radial velocity information is available for any

of the clusters and so kinematical criteria cannot be applied to refine the separation of the samples. We also note that our separation of the red LMC clusters into "globular" and "intermediate-age" objects has, interestingly, generated two groups whose luminosity distributions $\phi(V_t)$ are quite different. For the globulars, ϕ peaks symmetrically near $V_t \sim 11.3$ (cf Figure 6*c*), while for the other objects ϕ increases monotonically faintward. This is additional evidence—since V_t was not a classification parameter—that the red clusters contain more than one distinct population.

The populous blue $[(B-V) < 0.5]$ clusters in the LMC are often

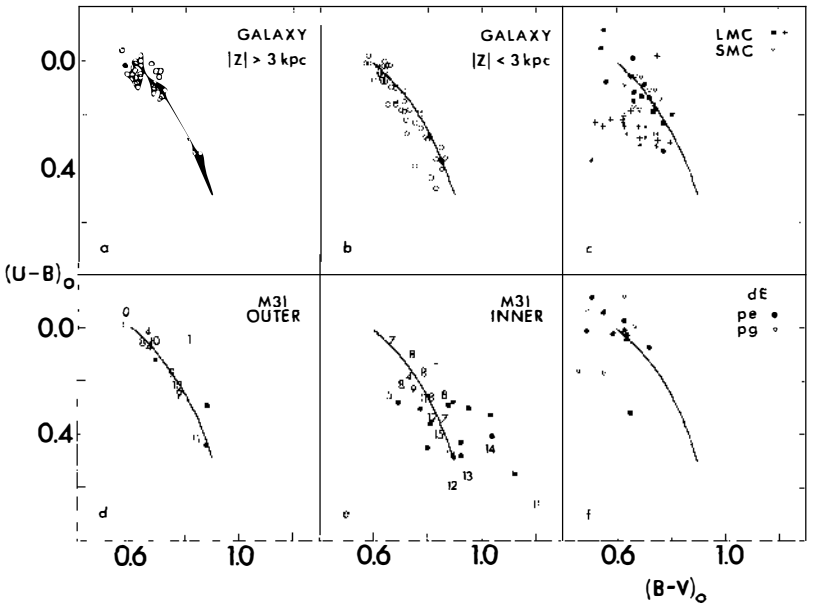

Figure 3 Color-color diagrams for globular cluster systems in the Local Group galaxies; all plotted points are photoelectric measurements except in panel (*f*). The intrinsic two-color line for the Galaxy (e.g. Racine 1973) is drawn in each panel. (*a*) Galactic globular clusters further than 3 kpc from the galactic plane. (*b*) Galactic globular clusters within 3 kpc of the plane; this sample contains most of the metal-rich clusters in the Galaxy. (*c*) Globular clusters in the Magellanic Clouds. Clusters in the LMC believed to be "nonglobular" (intermediate-age clusters or others; see text Section 2.1) are plotted as crosses. Clusters from Table 3 adopted as globular are plotted as open or closed symbols. (*d*) M31 globular clusters that lie outside the projected disk and are unreddened within M31 itself. Compare with panel (*a*). Those with measured line-strength index *L* (van den Bergh 1969) are plotted by their value of *L*. (*e*) M31 globular clusters seen projected on the M31 disk; compare with panel (*b*) for the analogous region in the Galaxy. (*f*) Globular clusters in the dwarf ellipticals NGC 147, 185, 205, and Fornax. Those with only photographic $U-B$ values are plotted as open symbols.

referred to as "young globular clusters" (Freeman 1974, Freeman & Munsuk 1973) in a stellar dynamical sense. Their ages are $\lesssim 10^8$ years, and some rival or exceed the brightest old globular clusters in luminosity. But their luminosities will fade with time as the upper main sequence evolves away. After 10^{10} yr, they will have dimmed by ~ 5 magnitudes (cf Larson & Tinsley 1978) and so will be much fainter and less conspicuous than the Cloud clusters which are *now* $\sim 10^{10}$ yr old. Thus by far the most massive Cloud clusters are just those that we have selected as globular, probably coeval with the Clouds themselves, and there appears no compelling evidence for believing that comparably massive clusters have formed since then.

Even for our restricted sample of old globulars in the Clouds, certain peculiarities in detail remain when compared with the Galactic globulars, which indicate residual differences in chemical composition or evolutionary characteristics. The same relation between CMD morphology and metallicity is not followed (cf the references cited); and three clusters (NGC 419, 1783, 1846)—sometimes considered globular (van den Bergh 1968) but rejected here on the basis of their integrated colors—possess extremely red stars at the tip of the giant branch (Feast & Lloyd-Evans 1973).

In Table 3, the 17 LMC clusters have a mean luminosity $\langle V_t \rangle = 11.21 \pm 0.27$ and the 13 SMC clusters have $\langle V_t \rangle = 11.82 \pm 0.30$. The 0.6 ± 0.4 mag difference between the two averages is consistent with the larger distance modulus of the SMC and with the assumption that the intrinsic luminosity distribution $\phi(M_V)$ is the same for both (Section 6.2 below). The LMC clusters display a significant range in intrinsic colors (Figure 3*c*) and hence presumably in metallicity. This is supported by the multiband photometry and line-strength indices of Danziger (1973), which also show substantial differences from cluster to cluster. By contrast, the SMC clusters have a much narrower color range and more uniform (lower) metallicity. However, no globular clusters in either Cloud are known to lie beyond the metallicity range seen in the Galactic globular clusters, and most fall in the range $-2 < [\mathrm{Fe/H}] < -1$.

In summary, it appears entirely possible to isolate a sample of clusters in both the LMC and SMC that occupies the familiar ranges of integrated color, luminosity, and approximate chemical composition and that we have defined as "globular." This rather crude classification of their properties will, however, doubtless be replaced by a much firmer analysis resulting from their current intensive study with the new large telescopes in the Southern Hemisphere.

Finally, we may roughly estimate the total expected number of "true" globular clusters in the Clouds under our operating criteria. In the LMC,

available photometric surveys of compact clusters reach $V \simeq 13.5$. Since most clusters of all kinds brighter than $V \sim 12.5$ have been observed, the present sample of 17 globulars should be 75% complete if their luminosity distribution resembles the one in the Galaxy. We adopt a total population $N_t = 23 \pm 5$. In the SMC, the larger distance is offset by its generally smoother background and the observers' efforts to push photometry somewhat deeper. A complete sample might therefore reach $N_t = 15 \pm 5$. These estimates are little more than educated guesses but will suffice for later discussion (Section 6.3).

3 THE ANDROMEDA GALAXY

3.1 *Fundamental Data*

Edwin Hubble (1932) first suggested that many of the small objects seen projected on the disk of M31 were its globular clusters. Walter Baade (1944a,b) later confirmed this identification through their incipient resolution on deep photographs. For entirely different reasons than in the Magellanic Clouds, the identification of a pure sample of globular clusters in M31 again presents an extremely difficult observational problem. Photographic images of the M31 clusters are less than 10 arc sec wide, and because their brightest stars are resolvable only in the best seeing conditions it is difficult to distinguish globular clusters from distant background spheroidal galaxies. Clusters projected against the irregular, patchy disk of M31 itself are additionally hard to distinguish, and can be confused with intermediate-age or compact young star clusters in the disk unless photometry or spectroscopy of their integrated light is available. Sargent et al. (1977) discuss in more detail the problems of image classification.

Hubble's original list of 140 objects was more than doubled with the later discoveries of many additional clusters by several authors (Seyfert & Nassau 1945, Mayall & Eggen 1953, Kron & Mayall 1960, Vetešnik 1962a,b, Baade & Arp 1964, Sharov 1973, 1976). The major recent survey of Sargent et al. (1977) yielded discoveries of many new clusters well out in the M31 halo. Sargent et al. also completely revised and compiled all previous lists of objects, eliminating known nonglobular clusters in the process (mainly by the selection criterion of diffuse and symmetric image structure, since no other useful data are available for most of these objects). Their final list contains 355 globular-cluster candidates on a uniform selection scale. Of these, eight are assigned to NGC 205 and we may reject 22 more whose UBV colors are too blue. Searle (1978) states that early results from spectrophotometry of a large subset of the Sargent et al. list indicate roughly 20% to be either background elliptical

galaxies (for the halo regions well away from the M31 disk) or intermediate-age clusters within the disk itself. In summary, we may therefore estimate that the Sargent et al. list, which includes all surveys to date, probably contains 300 ± 30 "true" globular clusters in the sense defined previously.

Photoelectric *UBV* measurements for 77 clusters (not all globular) are available from the combined work of Kron & Mayall (1960), Hiltner (1960), Kinman (1963), and van den Bergh (1969), while photographic photometry for a total of 246 is given by Vetešnik (1962a,b) and Racine (1965). We find the photometry of Sharov et al. (1976, 1977) and the photographic photometry of Kinman (1963) to contain sizeable systematic and random errors especially in the colors, and these are not used here. Comparison of the various photoelectric surveys shows satisfactory systematic agreement (to $0^m.03$ or better in all indices) and random errors in $V, (B-V)$ of $\sigma \simeq 0.07$, while the internal random errors of the averaged photographic data are roughly twice as large. After eliminating other types of objects from the photometric list, we are left with 188 out of the Sargent et al. survey that have *UBV* photometric indices.

The only other data yet available for a reasonably large number of M31 globular clusters are radial-velocity measurements for 43 objects and spectroscopic line-strength estimates for 37, both by van den Bergh (1969). Our current understanding of the kinematics and abundance structure of the M31 cluster system rests heavily on this single study. A major new velocity and abundance survey has been started by Searle (1978), which will eventually add considerably to both these areas.

3.2 *Systematic Properties*

Van den Bergh (1969) first indicated that the integrated colors of the M31 globular clusters—and by assumption their chemical composition—were distributed more heavily toward the red, metal-rich side and did not obey the same correlation in detail with galactocentric distance as in the Galaxy. Figure 3*d*,*e* displays the $(U-B, B-V)$ diagram for the M31 globular clusters with photoelectric color measurements, divided into two groups called "inner" (those projected on or near the M31 disk) and "outer" (those well beyond the disk and presumably unreddened within M31 itself). For comparison we show the same distribution for the Galactic globular clusters (data from Table 1), divided analogously into two "projected" spatial groups. Important differences between the two galaxies are immediately evident: the outer M31 clusters are more or less uniformly distributed over the full range of intrinsic colors; whereas few clusters redder than $(B-V)_0 \sim 0.75$ (or more metal-rich than $[\mathrm{Fe/H}] \sim -1$) are known in the outer Galaxy sample. The inner M31 clusters

display more scatter due to both larger photometric errors and effects of cluster reddening within M31, but their distribution suggests that this inner region may lack the blue, low-metallicity component [$(B-V) < 0.7$] that is known to extend right into the center of our own Galaxy (cf Figure 2). The mean intrinsic color of the outer M31 sample including only photoelectric measures and corrected for the M31 foreground reddening is $\langle B-V\rangle_0 = 0.74 \pm 0.02$, $\langle U-B\rangle_0 = 0.14 \pm 0.04$, which is slightly redder than the mean colors of the Galactic globular clusters at all radii ($\langle B-V\rangle_0 = 0.70 \pm 0.01$, $\langle U-B\rangle_0 = 0.13 \pm 0.01$).

The conclusion that the M31 clusters are more strongly weighted toward metal-richer objects is additionally supported by the distribution of the spectroscopic line-strength index L (van den Bergh 1969, also plotted in Figure 3*d*,*e*) as well as by the Searle (1978) spectrophotometry, scanner abundance studies, and Washington-system photometry for a small number of clusters (Spinrad & Schweizer 1972, Harris & Canterna 1977). Searle (1978) concludes that the mean abundance for the outer M31 sample is near [Fe/H] $\simeq -1.1$ as opposed to $\simeq -1.5$ for the outer Galaxy halo. In addition, plots of L or intrinsic color with projected galactocentric distance reveal no strong trend with distance, unlike what is observed within our Galaxy. However, the *very* strongest-line M31 clusters ($L > 11$, possibly including some with [Fe/H] > 0) are still found predominantly in the inner region.

The M31 cluster system is the only one outside the Galaxy for which statements can currently be made about *kinematics*. The cluster velocities measured by van den Bergh (1969) have been analyzed by Hartwick & Sargent (1974) to determine the velocity dispersion within the system and the total mass of M31 out to the radial limit of the survey. By dividing the sample into metallicity groups, they showed that the more metal-poor samples have the highest velocity dispersion, and that the total mass of M31 out to $r \sim 20$kpc is $\sim 3 \times 10^{11}\ \mathcal{M}_\odot$. Thus to first approximation the kinematics appear to resemble the Galactic cluster system.

Determining the intrinsic luminosity distribution $\phi(M_V)$ for the M31 clusters is impeded not only by the incompleteness and photometric errors mentioned, but by the necessity of making individual absorption corrections for reddening within M31 itself. To minimize the latter problem we have selected a sample consisting of 46 "outer" clusters (unreddened within M31) plus 68 "inner" clusters with low reddening [$(B-V) < 0.9$] for which photometry is available. Statistically corrected magnitudes $V_0 = V - 3[(B-V) - 0.82]$ were then used for the inner clusters since the photometric errors did not permit accurate individual dereddening. The resulting $\phi(M_V)$ histogram for 114 clusters is shown in Figure 6 and discussed further in Section 6.2. The faint-magnitude

incompleteness of the photometry causes a steep drop for $M_V > -6$, but the bright half is consistent with a peaked distribution with mode at $M_V \sim -7.5$.

Estimates of the true total number of M31 globular clusters must be made by taking the observed list of candidates (Sargent et al.) and correcting it for (*a*) contamination by background galaxies, old open clusters, etc., (*b*) incompleteness at faint magnitudes, and (*c*) incompleteness for the areas of the sky around M31 not yet surveyed. From the radial area distribution of the clusters (Section 6.3 below), we estimate that the area not covered by the Sargent et al. survey contains 35 ± 6 more clusters above the survey limit. The limiting magnitude itself is not accurately known but must be near $V \simeq 18$ ($M_V \simeq -6.6$). *If* $\phi(M_V)$ is the same in M31 and in the Galaxy (Figure 6 and Section 6.2) with the peak frequency at $\langle M_V \rangle \simeq -7.3$, then the observed M31 sample is only $\sim 70\%$ of the total over all magnitudes. Combining these corrections with the 20% fraction of contamination by other types of objects (Searle 1978) we finally estimate $N_t = 450 \pm 50$ as the total population of M31 globular clusters. This number exceeds the Galactic population ($N_t = 180 \pm 20$) by a factor of 2.5 ± 0.5. Though this ratio may be surprisingly large considering the roughly similar sizes of the two major Local Group spirals, it may simply indicate that the spheroidal component (central bulge and halo) is relatively more dominant in M31.

The projected density profile for the M31 globular-cluster system (cf Figure 8) follows a $r^{1/4}$ law in its outer region (de Vaucouleurs & Buta 1978; Section 6.3 here) but becomes increasingly flatter for $r < 3$ kpc. If this were due to increasing incompleteness of the Sargent et al. (1977) survey, then some 140 objects (70% of the expected total above the survey limit), including 20 brighter than $V = 16$, would have been missed in the extensively searched inner 30 arc min diameter area of M31. This much incompleteness appears highly unlikely. We conclude that, at least in part, the flattening of the density profile at $r < 3$ kpc is real.

4 DWARF GALAXIES

Aside from the two dominant large spirals and the Magellanic Clouds, other Local Group members that contain globular clusters of their own include the Sc spiral M33 and the dwarf ellipticals NGC 147, 185, 205, and Fornax. The available and rather meager information (in most cases including only *UBV* magnitudes and colors) for these systems is summarized in Table 4 and Figure 3*f*. The cluster identifications in Table 4 follow the authors cited below, and in the last column we give the projected galactocentric distances for each cluster.

Table 4 Globular clusters in dwarf galaxies

Galaxy	Cluster ID	V	$B-V$	$U-B$	r (kpc)
M 33	e	16.15	0.77	0.16	
	m	17.48	0.80	0.22	
	n	16.76	1.16	0.52	
	q	17.16	0.74	0.13	
	s	18.26	1.26	0.60	
	Mc	15.92	0.58	–	
Fornax	1	15.2:	0.51	0.03	2.1
	2	13.6	0.66	0.06	1.2
	3	12.5	0.65	0.03	0.8
	4	13.5	0.74	0.09	0.2
	5	13.4	0.61	0.04	2.1
	6	14.0:	–	–	0.3
NGC 147	I (H1)	17.66	0.80	0.45	0.0
	II (H2)	18.38			0.4
	III (H3)	16.98	0.64	0.00	0.7
	IV (H4)	21.10			0.3
NGC 185	I (H1)	18.38	0.79	0.15	0.6
	II (3)	19.7	0.94:	–	0.5
	III (H4, Bc)	16.78	0.69	0.06	0.2
	IV	–	–		0.7
	V (H5, Ba)	16.72	0.71	0.05	0.8
	VI	–	–		0.6
NGC 205	41 (H VIII)	16.68	0.58	0.00:	1.8
	51 (H V)	16.73	0.57	–	0.2
	54 (H IV)	18.52	0.51		0.2
	55	–	–	–	0.3
	56 (H VII)	17.24	0.76	0.06:	0.3
	57 (H VI)	17.86	0.72	−0.05:	0.2
	61 (H I)	16.80	0.55	0.23:	1.0
	63 (H II)	16.69	0.64	0.24:	0.6

In M33 the only published data remain the photometric surveys of Hiltner (1960) and Kron & Mayall (1960) for 23 selected clusters down to $V \sim 18.5$. Of these, most are open clusters of various ages, but three (e, m, and q) have color indices similar to normal metal-poor globular clusters. A possible fourth has no $(U-B)$ index, and two others have colors resembling highly reddened globular clusters. Scaling up Hiltner's discovery frequency of $\sim 5/23$ by the estimate that M33 contains ~ 100 clusters of all types (Kron & Mayall 1960) then yields the very uncertain prediction that M33 contains $N_t = 20 \pm 10$ true globular clusters. Much more observation will be needed before the clusters in this system are at all well understood.

The Fornax system is the largest dwarf spheroidal galaxy in the Local Group, but the smallest galaxy known to have globular clusters of its own (Hodge 1961, 1971b). For its six clusters *UBV* magnitudes and colors are available from the work of Hodge (1961, 1965, 1969), Kron & Mayall (1960), Demers (1969), and de Vaucouleurs & Ables (1970), as summarized in Table 4. It is interesting that even in such a small system, the clusters exhibit a noticeable range in metallicity, demonstrated by spectra and photometry of their integrated light (van den Bergh 1969, Danziger 1973, Harris & Canterna 1977). Cluster No. 4 has a metallicity approximately as high as M3, while the others appear to have much lower abundances, in the M92–M15 range. The color-magnitude diagrams for several of the clusters are currently under study by Demers and collaborators.

Hubble (1932) and Baade (1944a) made the first discoveries of clusters in the small elliptical galaxies surrounding M31. Currently, eight clusters are believed to belong to NGC 205 (Sargent et al. 1977). An additional cluster (H III), seen in projection against NGC 205, is assigned to the M31 system because of its high metallicity and discrepant radial velocity (van den Bergh 1969). Photoelectric $(B-V)$ colors of the clusters from the observations of Kron & Mayall (1960), van den Bergh (1969), and Hodge (1973) are summarized in Table 4, while the $(U-B)$ values listed are from the photographic data of Racine (1965) and Vetešnik (1962a).

From the surveys of Hodge (1976) and Ford et al. (1977), four clusters have been found in NGC 147. For these, useful photoelectric *UBV* colors are available for only two (Table 4), but magnitudes for all four.

In NGC 185 (which forms an optical pair with NGC 147, though Ford et al. 1977 argue that they are not physically bound), recent searches for globular clusters are described by Hodge (1974) and by Ford et al. (1977). Comparison of their two discovery lists suggests that NGC 185 contains perhaps six clusters (rejecting Hodge No. 2, and Ford et al. Nos. VII and VIII as probable galaxies). The available photoelectric photometry (Hodge 1974, Kron & Mayall 1960) for only four of them is again summarized in Table 4.

Photometry for most of the clusters in the three M31 companions is made uncertain by the varying background of their underlying galaxies and by the faintness of some of the clusters themselves. Nevertheless, the color indices (Figure 3*f*) suggest that all of their clusters fall near the bluer end of the intrinsic two-color line, and that in this sense they can be regarded as normal, metal-poor clusters. The present uncertainties in the data make it impossible to draw any further conclusions about the total range of abundances that each of these three galaxies has been able to generate in its clusters.

None of the several remaining small galaxies in the Local Group is definitely known to contain true globular clusters. The bright, compact dwarf elliptical M32 is superimposed on the disk of M31, making it impossible to identify any of the handful of M31 clusters in the area as belonging to M32. In any case, much of the M32 outer envelope has apparently been tidally stripped (Faber 1973, van den Bergh 1975) and so much of its hypothesized original cluster population may have been torn away.

The two faint irregulars NGC 6822 and IC 1613, according to Hodge (1977, 1978), are believed to lack globular clusters since the few cluster-like objects discovered in them resemble open clusters or the intermediate-age Magellanic Cloud clusters. The slightly more distant WLM irregular system (Ables & Ables 1977) does contain a single candidate, a surprisingly bright cluster at $M_B \simeq -9.2$, $(B-V)_0 \simeq 0.61$. However, whether this is a true globular cluster must await further data.

5 BEYOND THE LOCAL GROUP

5.1 *Globular Clusters in Virgo Galaxies*

Baum (1955) and Sandage (1961) discussed the numerous faint, stellar objects seen around the giant Virgo elliptical M87 as being its globular

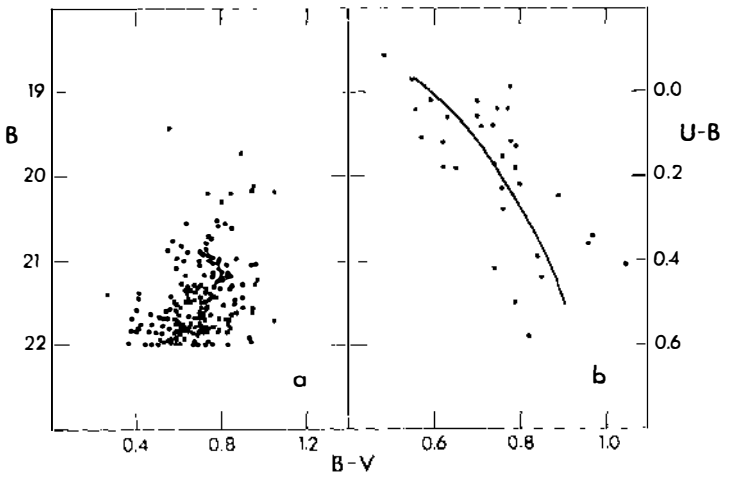

Figure 4 (*a*) Color-magnitude plot for 201 faint stellar objects around M87 with negligible proper motion ($\mu < 0''.005\ yr^{-1}$). Almost all these objects are M87 globular clusters, since the proper-motion criterion eliminates most foreground stars. (*b*) Color-color diagram for the M87 clusters; the intrinsic color line is the same as in Figure 3. The large observed range in intrinsic color is comparable with the M31 clusters (cf Figure 3*d*,*e*).

clusters, and Racine (1968a,b) first showed that their colors were consistent with this interpretation. Subsequent *UBV* photometric surveys of the M87 clusters were carried out by Hanes (1971) and by Ables et al. (1974). Figure 4 shows representative color-magnitude and color-color diagrams for 201 of these objects, where the *UBV* data are from Hanes (1971) and membership in M87 is confirmed by their negligible proper motion, $\mu < 0''.005$ yr^{-1} (Prociuk 1976). Though the color calibrations are still uncertain (cf Ables et al. 1974 and Hanes 1977b) the *UBV* colors fall in the same range as do the Local Group clusters (Figure 3). Hanes (1977a) also discussed the effects of observational errors on arguments for their photometric similarity. Spectrophotometry for three of the brightest clusters ($B \sim 21$) by Racine et al. (1978) indicates that their mean metallicity is higher than in the Galactic halo clusters and more nearly resembles the M31 halo instead.

For years M87 remained the only Virgo member about which anything concerning globular clusters was known. However, the recent single-color photometric survey by Hanes (1977b,c) for several more large Virgo galaxies, both ellipticals and spirals, demonstrated that globular clusters could indeed be found frequently in large numbers. Hanes' data concerning the luminosity distributions $\phi(m)$ and the total cluster populations in each Virgo galaxy, compared with the Local Group systems, will be discussed in more detail in Section 6. Most recently, programs to obtain *multicolor* photometry for large samples of clusters (and hence crude information about metallicity distributions in the halo of each galaxy) have been initiated by Harris and collaborators for three of the largest Virgo systems, M87, M49 (NGC 4472), and M104 (NGC 4594). Preliminary results for M87 alone indicate that the mean *UBVR* colors of the clusters decrease systematically from the center out to $r \sim 4$ arc min (25 kpc), and hence may represent an abundance gradient.

5.2 *Outside the Virgo System*

The Virgo galaxies quite obviously represent only a fraction of the cluster systems available for study beyond the Local Group. Several large E or S0 galaxies at roughly half the Virgo redshift including NGC 3115, 3377, 3379, 3384, and 4278 are noted to contain clusters (Sandage 1961, de Vaucouleurs & de Vaucouleurs 1965). These would be attractive to study particularly since they are ~ 1 mag closer than Virgo and provide correspondingly better chances to reach the turnover of the luminosity function. They may also yield further information on the relative effects of galaxy environment since none of them are members of large galaxy clusters. A preliminary single-color study of the clusters in NGC 3115 (Strom et al. 1977) indicates that their luminosity distribu-

Table 5 Globular-cluster systems in 27 galaxies

	Type	$(m-M)_V$	E_{B-V}	M_V	N_{obs}	N_t
Local Group						
M31	S	24.6	0.11	−21.1	300:	450
Galaxy	S	-	-	−20:	131	180
LMC	I	18.7	0.06	−18.5	17	23
SMC	I	19.1	0.04	−16.8	10	15
M33	S	24.5	0.03	−18.9	6	20
Fornax	dSph	21.0	0.02	−13.6	6	6
NGC 147	dE	24.6	0.15	−14.9	4	4
NGC 185	dE	24.6	0.15	−15.2	6:	7:
NGC 205	dE	24.6	0.11	−16.4	8	8
NGC 6822	I	24.2	0.30	−15.7	0	0
IC 1613	I	24.5	0.03	−14.8	0	0
WLM	I	26.2	0.06	−16.0	1:	1:

	Type	M_V	N_{obs}	N_t
Virgo System[a]				
NGC 4216	S	−21.0	21	520
NGC 4340	E	−19.9	26	650
NGC 4374 (M84)	E	−21.6	98	2500
NGC 4406 (M86)	E	−21.7	108	2600
NGC 4472 (M49)	E	−22.5	1700	4200
NGC 4486 (M87)	E	−22.3	6000	15000
NGC 4526	E	−21.3	87	2200
NGC 4564	E	−20.0	35	900
NGC 4569 (M90)	S	−21.4	32	800
NGC 4594 (M104)	S	−22.6	290	2800
NGC 4596	E	−20.4	82	2000
NGC 4621 (M59)	E	−21.1	63	1600
NGC 4636	E	−21.3	143	3600
NGC 4649 (M60)	E	−22.1	170	4200
NGC 4697	E	−21.6	72	1800

[a] $(m-M)_V = 30.9$, $E_{B-V} = 0.02$ assumed.

tion is at least roughly similar to that in M31 as it would be seen at 10 Mpc distance, which is consistent with the Hubble velocity of NGC 3115.

At distances well beyond Virgo, one is restricted to studying only the bright tip of the $\phi(M_V)$ distribution, and hence clusters can be detected only in the dominant giant ellipticals of great clusters (cf Section 6.1 below). Dawe & Dickens (1976) have apparently detected cluster systems in three of the largest ellipticals of the Fornax I cluster (NGC 1374, 1379, 1399), at $V_r \sim 1500$ km s^{-1} or 40% further than Virgo. Interestingly, they do not find noticeable numbers of clusters (to $B \simeq 22$) around several other comparably bright Fornax ellipticals. The present distance record is held for the giant elliptical NGC 3311 (in Hydra I) by Smith & Weedman (1976). Here the brightest clusters are seen to appear at $B \simeq 23.5$ and increase rapidly in number to the plate limit ($B \simeq 24$). Smith & Weedman conclude that the number of clusters (i.e. excess stellar images surrounding the galaxy) is again as expected if, for example M87 were displaced outward by 2.4 mag, corresponding to the observed ratio of the Hydra/Virgo recession velocities.

It remains a problem that virtually all the reliably established very distant globular-cluster systems are in large ellipticals, where they are of course most easy to detect. But this is the one galaxy type not represented in the Local Group, and detailed information about clusters in even one distant spiral galaxy would provide a much more rigorous basis for comparison with the Local Group.

6 GENERAL FEATURES OF GLOBULAR-CLUSTER SYSTEMS

6.1 *Total Populations and Dimensions of Parent Galaxies*

Table 5 summarizes available data on the number of actually observed globular clusters in 27 galaxies along with our estimated total populations N_t for each. Similar but less extensive data were discussed by Jaschek (1957) and Wakamatsu (1977b). Individual members of the Local Group were analyzed above. For Virgo galaxies Hanes' (1977a,b) counts were used, updated by the deeper ($B_{lim} \sim 24$) counting surveys of Harris & Smith (1976) for M87, of Harris & Petrie (1978) for M49, and of Harris et al. (1979) for M104. Virgo statistics are strongly dependent on the adopted field corrections; a new analysis of this question results in our quoted numbers (Table 5) being somewhat larger than the published net counts for M87. The total populations for M49, M87, and M104 were estimated from the limiting magnitude of the deep surveys, assuming V (peak) = 23.6 and $\sigma = 1\overset{m}{.}2$ for the luminosity distribution of Virgo globular clusters. Hanes's data for other galaxies were correspondingly

scaled up by the factor (25 ×) by which N_t for these three galaxies exceeded Hanes's field corrected counts. No other corrections for the limited angular field of the surveys have been applied, but these are expected to be small except for M87 (see Section 6.3).

The correlation between N_t and the luminosities of the parent galaxies is illustrated by Figure 5. Hanes (1977a) has already presented a discussion of this relation for Virgo galaxies. Over more than a factor of 1000, N_t for elliptical (E) galaxies is approximately proportional to the galaxy's luminosity. Spirals and irregulars are too bright for their estimated N_t. M31 would conform to the E relation had we adopted for M_V the luminosity of its spheroidal component (de Vaucouleurs 1958). Wakamatsu (1977b) has also shown that statistical reductions of other spiral luminosities to their spheroidal component produces similar results. This is, of course, because the luminous young stellar populations in the disk of spiral galaxies or in irregular systems represent a small fraction of the total mass of these galaxies and are genetically unrelated to globular clusters.

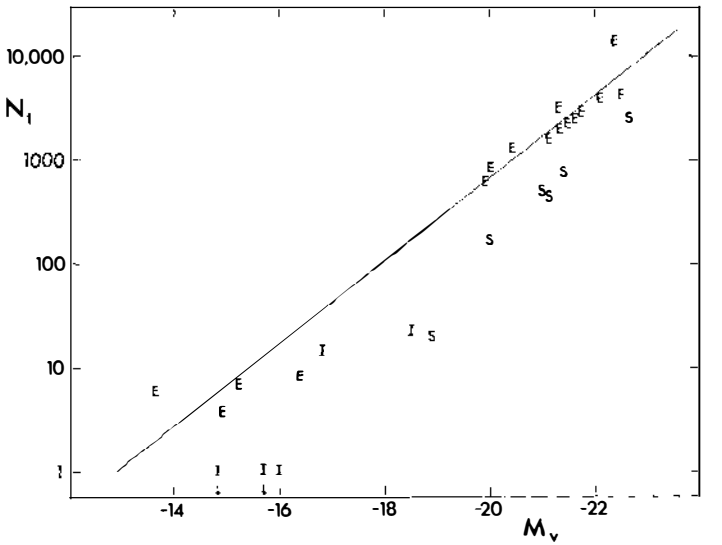

Figure 5 Correlation between the estimated total population of globular clusters N_t and the integrated absolute magnitude M_V of the parent galaxy. The different symbols are E for elliptical galaxies, S for spirals, and I for irregulars. The straight line represents direct proportionality between N_t and galaxy luminosity, as discussed in Section 6.1, and is drawn through the elliptical-galaxy sample. The spirals and irregulars all fall to the right of the line, presumably because their spheroidal (Population II) component represents only a fraction of their total luminosity (or mass).

Although Figure 5 might suggest that N_t is controlled by the total mass of the parent galaxy (cf Hanes 1977a), the data are not accurate enough to state that N_t is strictly proportional to L. The line $\log N_t = -0.4$ $(M_V - 12.9)$ is shown in the figure; this relation implies that globular clusters contribute approximately one half of one per cent of the total light of E galaxies. According to Faber & Jackson (1976) the mass-to-light ratio $\mathcal{M}/L$ for spheroidal galaxies tends to vary as $L^{1/2}$. If N_t were strictly proportional to $\mathcal{M}_{gal}$ this would require $\log N_t \propto 0.6\ M_V$. This is not consistent with the correlation shown in Figure 5. One could speculate that dwarf elliptical galaxies are more efficient progenitors of globular clusters—having similar $\mathcal{M}/L \sim 2$ (Hodge 1971b, Illingworth 1976). Alternatively they may have lost a large fraction of the initial mass they had when their globular clusters were formed.

M87 has many more globular clusters for its luminosity than normal E galaxies. Evidence that our estimate of N_t (M87) is still too low will be presented later. The extremely large population of globular clusters in M87 could be due to its privileged central position and low peculiar velocity in the Virgo cluster (van den Bergh 1977b). Alternatively, the M87 mass-to-light ratio may be abnormally large (Harris & Petrie 1978).

6.2 *Luminosity Functions*

The brightest globular clusters are more luminous than any other stellar "standard candles" except supernovae and have long been potentially attractive extragalactic distance indicators. Their fundamental advantages for this purpose are well described by Hanes (1977b), and current agreements or disagreements with other recent methods for calibrating the Hubble constant are well known (Tammann 1976, Fisher & Tully 1977, Peebles 1978). Only a brief discussion of the present state of the globular-cluster technique can be given here.

Early attempts to calibrate the Virgo distance by assuming a fixed luminosity for the brightest clusters in the Galaxy, M31 and M87 (Baum 1955, Sandage 1968, Racine 1968b), later failed when it was established that this maximum luminosity depended on galaxy size (de Vaucouleurs 1970, Harris 1974, Hodge 1974, Hanes 1977b,c). De Vaucouleurs (1977b, 1978) has demonstrated how a population-corrected brightest-cluster method can still be used. But ideally one should calibrate the intrinsic magnitudes of the clusters in a distant galaxy by fitting their *entire* observed luminosity distribution $\phi(m)$ to the familiar nearby galaxies.

The raw $\phi(M_V)$ distributions for Local Group galaxies are displayed in Figure 6. The four dE's are lumped together as are the two Magellanic Clouds, and the M31 sample is restricted to 114 clusters of low reddening as described in Section 3.2. For the Galaxy the distribution is seen to

conveniently match a Gaussian curve (de Vaucouleurs 1970, 1977b, Hanes 1977b,c), although we emphasize that no compelling reason exists to adopt this model as *physically* real. The curve shown in Figure 6 has its peak at $\langle M_V \rangle = -7.3 \pm 0.1$ and dispersion $\sigma_V = 1.20 \pm 0.05$. A least-squares fit to the Galaxy data points for $M_V < -6.0$ (93 clusters) in the manner described by Hanes (1977c) yields a Gaussian with $\langle M_V \rangle = -7.34$, $\sigma_V = 1.17$, while adding the dE and the Magellanic Clouds samples to the Galaxy (139 clusters total) gives $(-7.28, 1.23)$. Applying the same Gaussian curve to the other Local Group members in Figure 6, we conclude that within the current uncertainties the hypothesis of a universal $\phi(M)$ for globular clusters is entirely reasonable for a remarkably wide range of parent galaxy types. Only the faint half of the M31 data, which is certainly incomplete, deviates significantly.

Figure 7 summarizes the totality of present $\phi(m)$ data by showing a fit of Virgo to the Local Group (cf Hanes 1979). To the Hanes data we have added two points on the integral $N(m)$ curve derived from deeper cluster counts in M87 (Harris & Smith 1976) and in M49 (Harris & Petrie

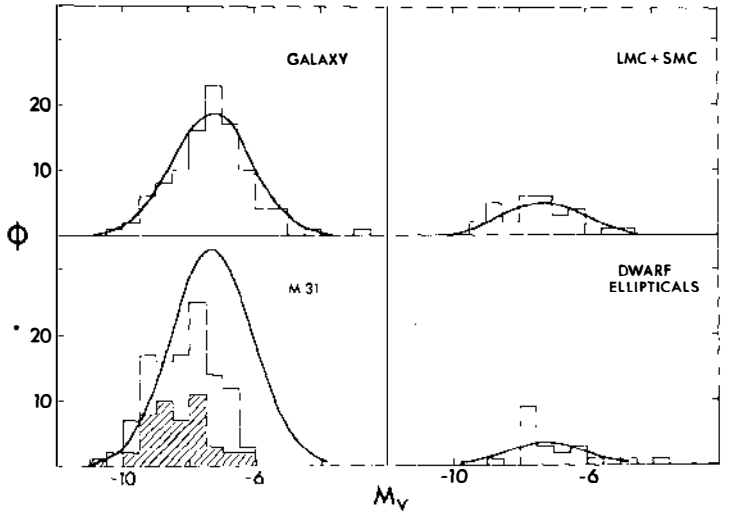

Figure 6 Luminosity distributions for globular-cluster systems in the Local Group galaxies. Here $\phi(M_V)$ is the number of clusters found in each half-magnitude interval for each galaxy sample. Gaussian model curves of peak $\langle M_V \rangle = -7.3$ and standard deviation $\sigma = 1.2$ mag are superimposed, suitably scaled to match the total cluster population N in each galaxy. For M31, the data are progressively more incomplete for $M_V \gtrsim -8$ (see text Section 6.2) and its curve is normalized to $N \simeq 200$. Here the shaded area of the histogram represents the 48 unreddened "outer" M31 clusters, and the unshaded part represents the 76 little-reddened clusters in the disk.

1978). These new counts reach one magnitude fainter than Hanes's limit and, being much closer to the peak of the $\phi(M_V)$ curve, provide a stronger constraint on the choice of the Virgo distance modulus. In Figure 7 we have more or less arbitrarily assumed $(m-M)_{V,\,\mathrm{Virgo}} = 30.9 \pm 0.3$, corresponding to $H_0 = 75 \pm 10$ km s^{-1} Mpc^{-1}. The overall quality of the fit supports the assertion that at least the *shape* of the $\phi(M)$ curve is similar in all galaxies. The significant curvature of the mean line in this log-log plot shows also that $\phi(M)$ is not well fitted by a power law as has been claimed elsewhere (Tremaine et al. 1975, Tremaine 1976). As Hanes (1977c) emphasizes, it is important to realize that the distance fit can be carried out independently of the Gaussian model, although both the Local Group and the Virgo data fit this model satisfactorily.

We conclude that the observational evidence supports the concept of a universal luminosity function for globular clusters and that $\phi(m)$ is

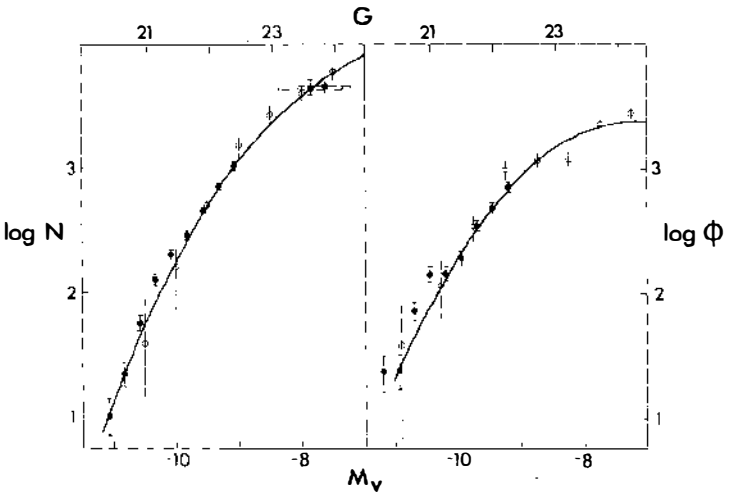

Figure 7 Fit of the Local Group luminosity function $\phi(M_V)$ to the Virgo system. Open circles denote the Local Group data combining ϕ for the Galaxy, dwarf ellipticals, Magellanic Clouds, and M31 (the latter corrected for incompleteness for $M_V > -8$). Closed circles represent the combined data for 6 giant Virgo ellipticals with the largest cluster populations (Hanes 1977c). The two populations have been fit assuming $(m-M)_V$ (Virgo) = 30.9, and the scale at top represents the corresponding apparent blue magnitudes G of Hanes's data. (*a*) The integrated luminosity function $N(M_V)$ (number of clusters brighter than M_V). Internal error bars are indicated for each data set, and the Gaussian model line described previously is drawn in. All the Virgo points for $G < 23$ are from Hanes (1977c), whereas the two extra points at upper right represent the Harris/Smith and Harris/Petrie cluster counts around M87 and M49, normalized to the same field size as the Hanes data. (*b*) The differential luminosity function $\phi(M_V)$ as defined in Figure 6, with the Gaussian curve again drawn in.

indeed a potentially important distance indicator in extragalactic studies. A crucial future test will be to observe the turnover of $\phi(m)$ in Virgo, which should occur at $V \sim 23.5$ if the present argument is correct.

6.3 *Density Profiles*

Figure 8 shows the projected density profile of four globular-cluster systems for which comprehensive data are available (Harris 1976, Sargent et al. 1977, Harris & Smith 1976, Harris & Petrie 1978). The outer regions of all these profiles are adequately represented by a de Vaucouleurs (1977a) $R^{1/4}$ law. They illustrate in a dramatic way the huge range in the characteristic sizes of globular-cluster systems. The $R^{1/4}$ lines drawn in Figure 8 have the following equations and effective radii R_e (Young 1976):

for the Galaxy, $\log \sigma = 3.4 - 2.57\, R^{1/4}$, $R_e = 3$ kpc,
for M31, $\log \sigma = 3.1 - 2.03\, R^{1/4}$, $R_e = 7$ kpc,
for M49, $\log \sigma = 2.7 - 1.33\, R^{1/4}$, $R_e = 40$ kpc,
and for M87, $\log \sigma = 2.5 - 1.05\, R^{1/4}$, $R_e = 100$ kpc.

For each galaxy the zero points of $\log \sigma$ have been normalized to the total population N_t (Table 5) of the area surveyed. The quoted slope for the Galaxy is the same as de Vaucouleurs' (1977a). For M31, our corrections

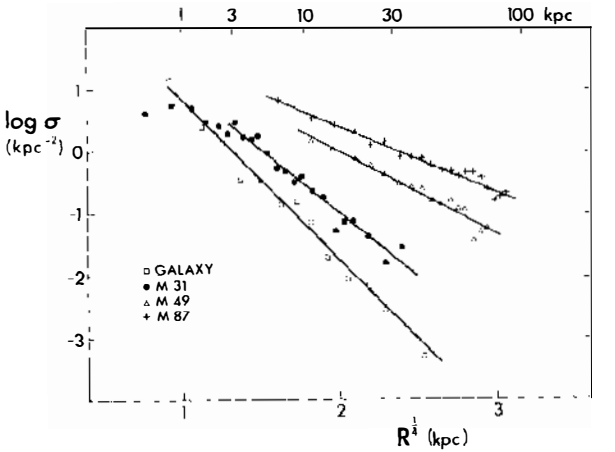

Figure 8 The radial density distribution of globular clusters in four major galaxies. Here σ is the number of clusters per kpc^2, plotted against projected galactocentric distance R in kpc. The data sources are Harris (1976, for the Galaxy), Sargent et al. (1977, and Section 3.2 for M31), Harris & Petrie (1978, for M49), and Harris & Smith (1976, for M87). The linear fits drawn through each distribution are the $R^{1/4}$ relations described in Section 6.3. Note the inner M31 points, which fall well below the $R^{1/4}$ curve, and also the vastly different scale sizes of each system.

for incompleteness of the survey (Section 3.2) at $R > 15$ kpc lead to a shallower profile, and hence a larger R_e, than obtained by de Vaucouleurs & Buta (1978).

The smaller size of the Galaxy's system would favor a type Sc rather than Sb for the Galaxy. The two gE systems have much larger R_e's than do the two spirals, and the M87 system is so large that our current estimate of $N_t = 15{,}000$ (Section 6.1) for $R < 90$ kpc may still fail to account for all its clusters by a factor of two or more. If no tidal radius limits the extent of this system, the M87 globular clusters would span much of the whole central Virgo cluster ($R \sim 1$ Mpc) before their projected density would drop to the level found in the outer halo of our Galaxy. Perhaps it will become preferable to think of these tens of thousands of globular clusters surrounding the central giant galaxy M87 as a system associated with the Virgo cluster itself!

A comparison of the density profiles in Figure 8 with the photometric profiles of the spheroidal components of M31 (de Vaucouleurs 1958), of M49 (King 1978a, Harris & Petrie 1978), and of M87 (de Vaucouleurs & Nieto 1978, King 1978a, Oemler 1976) reveals that the globular cluster systems have significantly larger characteristic sizes (shallower slopes) than do the parent galaxies. In earlier discussions (Harris & Smith 1976, Wakamatsu 1977a, Harris & Petrie 1978) it had been conventional to ascribe discrepant slopes between the cluster system and the halo integrated light to incompleteness of cluster counts (central regions) or to uncertain background corrections (outer regions). But the background counts are now better known, and, as has already been discussed for M31 (Section 3.2), the central regions would have many easily detectable bright clusters if the incompleteness fractions were as high as had been claimed. Our conclusion is therefore that the effect is at least partly real. This may indicate that globular clusters were formed at an earlier epoch than were the stars of the spheroidal component of galaxies, i.e. at a time when the protogalactic material was less centrally condensed.

As a final conclusion we may emphasize the impressive similarities displayed by systems of globular clusters in a vast diversity of galaxies. These systems appear to be inherently simple. Their total population is purely a function of the spheroidal mass of the parent galaxy; their density profiles are homologous, following the same law that applies to the simplest elliptical galaxies; they apparently share a unique luminosity (mass) function. Each individual system also presents peculiarities (notably in its metallicity characteristics) but here again some universal trends with galaxy mass or type are beginning to show. The overall picture of universality that emerges from this review suggests to us that as one learns more about globular clusters in galaxies, one uncovers important aspects

of the earliest differentiated structures in the Universe—aspects of an epoch that initiated the birth of the galaxies themselves and that was not far removed from the primary instant of the Universe.

Literature Cited

Ables, H. D., Ables, P. G. 1977. *Ap. J. Suppl.* 34:245
Ables, H. D., Newell, E. B., O'Neil, E. J. 1974. *Publ. Astron. Soc. Pac.* 86:311
Alcaino, G. 1977a. *Astron. Astrophys. Suppl.* 27:255
Alcaino, G. 1977b. *Publ. Astron. Soc. Pac.* 89:491
Alcaino, G. 1978a. *Astron. Astrophys. Suppl.* 33:181
Alcaino, G. 1978b. *Astron. Astrophys. Suppl.* 34:431
Arp, H. C. 1958. *Astron. J.* 63:487
Arp, H. C. 1965. In *Galactic Structure*, ed. A. Blaauw, M. Schmidt, p. 401. Univ. Chicago Press, Ill. 606 pp.
Baade, W. 1944a. *Ap. J.* 100:137
Baade, W. 1944b. *Ap. J.* 100:147
Baade, W., Arp, H. C. 1964. *Ap. J.* 139:1027
Baum, W. A. 1955. *Publ. Astron. Soc. Pac.* 67:328
Bell, R. A., Gustafsson, B. 1976. In *The Galaxy and the Local Group*, ed. R. J. Dickens, J. E. Perry. *RGO Bull. No. 182*
Bernard, A. 1975. *Astron. Astrophys.* 40:199
Bernard, A. 1976. *Astron. Astrophys. Suppl.* 25:281
Bigay, J. H., Bernard, A. 1974. *Astron. Astrophys.* 33:123
Bok, B. J. 1966. *Ann. Rev. Astron. Astrophys.* 4:95
Butler, D. 1975. *Ap. J.* 200:68
Canterna, R., Schommer, R. 1978. *Ap. J. Lett.* 219:L119
Christie, W. H. 1940. *Ap. J.* 91:8
Cohen, J. 1978. *Ap. J.* 223:487
Corwin, H. G. 1977. *Astron. J.* 82:193
Cowley, A. P., Hartwick, F. D. A., Sargent, W. L. W. 1978. *Ap. J.* 220:453
Da Costa, G. S., Freeman, K. C., Kalnajs, A. J., Rodgers, A. W., Stapinski, T. E. 1977. *Astron. J.* 82:810
Danziger, I. J. 1973. *Ap. J.* 181:641
Dawe, J. A., Dickens, R. J. 1976. *Nature* 263:395
Delhaye, J. 1965. In *Galactic Structure*, ed. A. Blaauw, M. Schmidt, p. 61. Chicago: Univ. Chicago Press. 606 pp.
Demarque, P., McClure, R. D. 1977. In *The Evolution of Galaxies and Stellar Populations*, ed. B. M. Tinsley, R. B. Larson, p. 199. Yale Univ. Obs. 449 pp.
Demers, S. 1969. *Astrophys. Lett.* 3:175
de Vaucouleurs, G. 1958. *Ap. J.* 128:465
de Vaucouleurs, G. 1970. *Ap. J.* 159:435
de Vaucouleurs, G. 1977a. *Astron. J.* 82:456
de Vaucouleurs, G. 1977b. *Nature* 266:126
de Vaucouleurs, G. 1978. *Ap. J.* 224:14
de Vaucouleurs, G., Ables, H. D. 1970. *Ap. J.* 159:425
de Vaucouleurs, G., Buta, R. 1978. *Astron. J.* 83:1383
de Vaucouleurs, G., de Vaucouleurs, A. 1965. *Reference Catalog of Bright Galaxies.* Austin: Univ. Texas Press. 1st ed.
de Vaucouleurs, G., Nieto, J. L. 1978. *Ap. J.* 220:449
Diamond, G. E. 1976. MSc thesis. Univ. Toronto
Eggen, O. J., Lynden-Bell, D., Sandage, A. 1962. *Ap. J.* 136:748
Faber, S. M. 1973. *Ap. J.* 179:423
Faber, S. M., Jackson, R. E. 1976. *Ap. J.* 204:668
Feast, M. W., Lloyd-Evans, T. 1973. *MNRAS* 164:15P
Fisher, J. R., Tully, R. B. 1977. *Comments Astrophys. Space Sci.* 7:85
Ford, H. C., Jacoby, G., Jenner, D. C. 1977. *Ap. J.* 213:18
Freeman, K. C. 1974. In *Proc. ESO/SRC/CERN Conf. Research Programmes for Large Telescopes*, ed. A. Reiz, p. 177
Freeman, K. C., Gascoigne, S. C. B. 1977. *Proc. Astron. Soc. Aust.* 3:136
Freeman, K. C., Munsuk, C. 1973. *Proc. Astron. Soc. Aust.* 2:151
Gascoigne, S. C. B. 1966. *MNRAS* 134:59
Gascoigne, S. C. B. 1971. In *The Magellanic Clouds*, ed. J. Muller, p. 25. Dordrecht, Holland: Reidel
Gascoigne, S. C. B., Burr, E. J. 1956. *MNRAS* 116:570
Gascoigne, S. C. B., Kron, G. E. 1952. *Publ. Astron. Soc. Pac.* 64:196
Gascoigne, S. C. B., Lynga, G. 1963. *Observatory* 83:38
Goodenough, D. G., Hartwick, F. D. A. 1970. *Publ. Astron. Soc. Pac.* 82:921
Gratton, R. G., Nesci, R. 1978. *MNRAS* 182:61P
Gray, D. F. 1965. *Astron. J.* 70:362
Hanes, D. A. 1971. MSc thesis. Univ. Toronto
Hanes, D. A. 1977a. *MNRAS* 179:331
Hanes, D. A. 1977b. *Mem. R. Astron. Soc.* 84:45
Hanes, D. A. 1977c. *MNRAS* 180:309

Hanes, D. A. 1979. *MNRAS*. In press
Harris, H. C., Canterna, R. 1977. *Astron. J.* 82:798
Harris, W. E. 1974. PhD thesis. Univ. Toronto
Harris, W. E. 1976. *Astron. J.* 81:1095
Harris, W. E. 1977. *Publ. Astron. Soc. Pac.* 89:482
Harris, W. E. 1978. *Publ. Astron. Soc. Pac.* 90:45
Harris, W. E., Canterna, R. 1979a. Submitted for publication
Harris, W. E., Canterna, R. 1979b. *Ap. J. Lett.* 231. In press
Harris, W. E., Hesser, J. E. 1976. *Publ. Astron. Soc. Pac.* 88:377
Harris, W. E., Petrie, P. L. 1978. *Ap. J.* 223:88
Harris, W. E., Smith, M. G. 1976. *Ap. J.* 207:1036
Harris, W. E., Smith, M. G., van den Bergh, S. 1979. In preparation
Harris, W. E., van den Bergh, S. 1974. *Astron. J.* 79:31
Hartwick, F. D. A. 1976. *Ap. J.* 209:418
Hartwick, F. D. A., Cowley, A. P. 1978. Paper delivered at *NATO Adv. Study Inst. on Globular Clusters*. Cambridge Univ.
Hartwick, F. D. A., Sargent, W. L. W. 1974. *Ap. J.* 190:283
Hartwick, F. D. A., Sargent, W. L. W. 1978. *Ap. J.* 221:512
Helfer, H. L., Wallerstein, G., Greenstein, J. L. 1959. *Ap. J.* 129:700
Hesser, J. E., Hartwick, F. D. A., McClure, R. D. 1977. *Ap. J. Suppl.* 33:471
Hesser, J. E., Hartwick, F. D. A., Ugarte, P. 1976. *Ap. J. Suppl.* 32:283
Hiltner, W. A. 1960. *Ap. J.* 131:163
Hodge, P. W. 1960a. *Ap. J.* 131:351
Hodge, P. W. 1960b. *Ap. J.* 132:346
Hodge, P. W. 1961. *Astron. J.* 66:83
Hodge, P. W. 1965. *Ap. J.* 141:308
Hodge, P. W. 1969. *Publ. Astron. Soc. Pac.* 81:875
Hodge, P. W. 1971a. *Smithsonian Astrophys. Obs. Spec. Rep. No. 337*
Hodge, P. W. 1971b. *Ann. Rev. Astron. Astrophys.* 9:35
Hodge, P. W. 1973. *Ap. J.* 182:671
Hodge, P. W. 1974. *Publ. Astron. Soc. Pac.* 86:289
Hodge, P. W. 1976. *Astron. J.* 81:25
Hodge, P. W. 1977. *Ap. J. Suppl.* 33:69
Hodge, P. W. 1978. *Ap. J. Suppl.* 37:145
House, F., Wiegandt, R. 1977. *Astrophys. Space Sci.* 48:191
Hubble, E. 1932. *Ap. J.* 76:44
Illingworth, G. 1976. *Ap. J.* 204:73
Innanen, K. A. 1967. *Z. Astrophys.* 64:445
Innanen, K. A., Valtonen, M. J. 1977. *Ap. J.* 214:692
Jaschek, C. O. R. 1957. *Z. Astrophys.* 44:33
Jenner, D. C., Kwitter, K. B. 1977. *Bull. Am. Astron. Soc.* 9:287
Johnson, H. L. 1959. *Lowell Obs. Bull.* 4:117
Keenan, D. W. 1978. Paper delivered at *NATO Adv. Study Inst. on Globular Clusters*. Cambridge Univ.
King, I. R. 1962. *Astron. J.* 67:471
King, I. R. 1966a. *Astron. J.* 71:64
King, I. R. 1966b. *Astron. J.* 71:276
King, I. R. 1978a. *Ap. J.* 222:1
King, I. R. 1978b. *NATO Adv. Study Inst. on Globular Clusters*. Cambridge Univ.
Kinman, T. D. 1959a. *MNRAS* 119:157
Kinman, T. D. 1959b. *MNRAS* 119:538
Kinman, T. D. 1959c. *MNRAS* 119:559
Kinman, T. D. 1963. *Ap. J.* 137:213
Kron, G. E. 1956. *Publ. Astron. Soc. Pac.* 68:230
Kron, G. E. 1966. *Publ. Astron. Soc. Pac.* 78:143
Kron, G. E. 1975. Private communication
Kron, G. E., Guetter, H. H. 1976. *Astron. J.* 81:817
Kron, G. E., Mayall, N. U. 1960. *Astron. J.* 65:581
Kukarkin, B. V. 1974. *The Globular Star Clusters*. Sternberg State Astron. Inst. Moscow: Nauka. 135 pp.
Kurth, R. 1960. *Z. Astrophys.* 50:215
Larson, R. B. 1975. *MNRAS* 173:671
Larson, R. B. 1976. *MNRAS* 176:31
Larson, R. B., Tinsley, B. M. 1978. *Ap. J.* 219:46
Lee, S. W. 1977a. *Astron. Astrophys. Suppl.* 27:367
Lee, S. W. 1977b. *Astron. Astrophys. Suppl.* 28:409
Lee, S. W. 1977c. *Astron. Astrophys. Suppl.* 29:1
Lightman, A. P., Shapiro, S. L. 1978. *Rev. Mod. Phys.* 50:437
Liller, M. H., Carney, B. W. 1978. *Ap. J.* 224:383
Liller, W. 1977. *Ap. J. Lett.* 213:L21
Lindsay, E. M. 1956. *Irish Astron. J.* 4:65
Lindsay, E. M. 1958. *MNRAS* 118:172
Mallia, E. A. 1977. *Astron. Astrophys.* 60:195
Matsunami, N. 1963. *Publ. Astron. Soc. Jap.* 16:141
Mayall, N. U. 1946. *Ap. J.* 104:290
Mayall, N. U., Eggen, O. J. 1953. *Publ. Astron. Soc. Pac.* 65:24
Morgan, W. W. 1956. *Publ. Astron. Soc. Pac.* 68:509
Oemler, G. 1976. *Ap. J.* 209:693
Oort, J. H. 1977. *Ap. J. Lett.* 218:L97
Ostriker, J. P., Spitzer, L., Chevalier, R. A. 1972. *Ap. J. Lett.* 176:L51
Peebles, P. J. E. 1978. *Comments Astrophys. Space Sci.* 7:197

Peterson, C. J. 1974. *Ap. J. Lett.* 190:L17
Peterson, C. J. 1976. *Astron. J.* 81:617
Peterson, C. J., King, I. R. 1975. *Astron. J.* 80:427
Prociuk, I. 1976. MSc thesis. Univ. Toronto
Racine, R. 1965. MSc thesis. Univ. Toronto
Racine, R. 1968a. *Publ. Astron. Soc. Pac.* 80:326
Racine, R. 1968b. *J. R. Astron. Soc. Can.* 62:367
Racine, R. 1973. *Astron. J.* 78:180
Racine, R. 1975. *Astron. J.* 80:1031
Racine, R., Harris, W. E. 1975. *Ap. J.* 196:413
Racine, R., Oke, J. B., Searle, L. 1978. *Ap. J.* 223:82
Rousseau, J. 1964. *Ann. Astrophys.* 27:681
Rutily, B., Terzan, A. 1977. *Astron. Astrophys. Suppl.* 30:315
Sandage, A. 1961. *The Hubble Atlas of Galaxies. Carnegie Inst. Washington Publ. No. 618.* Washington DC
Sandage, A. R. 1968. *Ap. J. Lett.* 152:L149
Sandage, A. R., Hartwick, F. D. A. 1977. *Astron. J.* 82:459
Sandage, A., Katem, B., Johnson, H. L. 1977. *Astron. J.* 82:389
Sargent, W. L. W., Kowal, S. T., Hartwick, F. D. A., van den Bergh, S. 1977. *Astron. J.* 82:947
Saslaw, W. C. 1973. *Publ. Astron. Soc. Pac.* 85:5
Sawyer, H. B., Shapley, H. 1927. *Harvard Coll. Obs. Bull. No. 848*
Sawyer Hogg, H. B. 1959. *Handbuch der Physik*, ed. S. Flugge, 53:129. Berlin: Springer
Schmidt, M. 1956. *Bull. Astron. Inst. Neth.* 13:15
Schmidt, M. 1965. See Arp, 1965, p. 513
Schuster, H. E., West, R. M. 1977. *The Messenger*, No. 10, p. 13
Searle, L. 1978. Paper delivered at *NATO Adv. Study Inst. on Globular Clusters.* Cambridge Univ.
Searle, L., Zinn, R. 1978. *Ap. J.* 225:357
Seyfert, C. K., Nassau, J. J. 1945. *Ap. J.* 102:377
Shapley, H. 1918. *Ap. J.* 48:89
Sharov, A. S. 1973. *Sov. Astron.—AJ* 17:174
Sharov, A. S. 1976. *Sov. Astron.—AJ* 20:397
Sharov, A. S., Lyutyi, V. M., Esipov, V. F. 1976. *Sov. Astron. Lett.* 1:69
Sharov, A. S., Lyutyi, V. M., Esipov, V. F. 1977. *Sov. Astron. Lett.* 2:128
Smith, M. G., Hesser, J. E., Shawl, S. J. 1976. *Ap. J.* 206:66
Smith, M. G., Weedman, D. W. 1976. *Ap. J.* 205:709
Spinrad, H., Schweizer, F. 1972. *Ap. J.* 171:403
Spitzer, L. 1958. *Ap. J.* 127:17
Strom, K. M., Strom, S. E., Jensen, E. B., Moller, J., Thompson, L. A., Thuan, T. X. 1977. *Ap. J.* 212:335
Surdin, V. G., Charikov, A. V. 1977. *Sov. Astron.—AJ* 21:12
Tammann, G. A. 1976. See Bell & Gustaffson 1976. p. 136
Tifft, W. G. 1962. *MNRAS* 125:199
Tremaine, S. 1976. *Ap. J.* 203:345
Tremaine, S. D., Ostriker, J. P., Spitzer, L. 1975. *Ap. J.* 196:407
van de Kamp, P. 1964. *Elements of Astromechanics.* San Francisco: Freeman. 133 pp.
van den Bergh, S. 1967. *Astron. J.* 72:70
van den Bergh, S. 1968. *J. R. Astron. Soc. Can.* 62:145, 219
van den Bergh, S. 1969. *Ap. J. Suppl.* 19:145
van den Bergh, S. 1971. *Astron. J.* 76:1082
van den Bergh, S. 1975. *Ann. Rev. Astron. Astrophys.* 13:217
van den Bergh, S. 1977a. *Astron. J.* 82:796
van den Bergh, S. 1977b. *Vistas Astron.* 21:71
van den Bergh, S. 1978. Paper delivered at *NATO Adv. Study Inst. on Globular. Clusters.* Cambridge Univ.
van den Bergh, S., Hagen, G. L. 1968. *Astron. J.* 72:569
Vetešnik, M. 1962a. *Bull. Astron. Inst. Czech.* 13:180
Vetešnik, M. 1962b. *Bull. Astron. Inst. Czech.* 13:218
von Hoerner, S. 1955. *Z. Astrophys.* 35:255
Wakamatsu, K. I. 1977a. *Publ. Astron. Soc. Pac.* 89:267
Wakamatsu, K. I. 1977b. *Publ. Astron. Soc. Pac.* 89:504
Walker, M. F. 1970. *Ap. J.* 161:835
Walker, M. F. 1972. *MNRAS* 156:459
Woltjer, L. 1975. *Astron. Astrophys.* 42:109
Woolley, R. v. d. R. 1961. *Observatory* 81:161
Young, P. J. 1976. *Astron. J.* 81:807
Zaitseva, G. V., Lyutyi, V. M., Kukarkin, B. V. 1974. *Sov. Astron.—AJ* 18:257
Zinn, R. 1974. *Ap. J.* 193:593

Annual Review of Astronomy and Astrophysics
Volume 17, 1979

CONTENTS